Acute targeted induction of gut-microbial metabolism affects host clock genes and nocturnal feeding

Giorgia Greter[1*], Claudia Moresi[1], Stefanie Oswald[1], Alice de Wouters d'Oplinter[1], Daria Künzli[1], Elisa Cappio Barazzone[1], Jiayi Lan[2], Emma Slack[1], Markus Arnoldini[1*]

[1]Department of Health Sciences and Technology, ETH Zurich, 8093, Zurich, Switzerland

[2]Department of Chemistry and Applied Biosciences, ETH Zurich, 8093, Zurich, Switzerland

---

Summary

The gut microbiota and host circadian clock mutually influence each other, and microbiota metabolism has been shown to play a role in regulating host circadian function via secretion of fermentation products. Microbial metabolism is dependent on the availability of nutrients for the microbiota, typically through the host's food intake, making it challenging to disentangle the effect of host and microbiota metabolism. In this study, we acutely induced gut microbial metabolic activity without inducing host metabolism in mice. We found that increasing microbial metabolism in the gut altered circadian clock gene expression locally. Actuating microbiota metabolism also reduced host food intake beyond the calories provided by the microbiota, suggesting a systemic signaling effect of microbial metabolism on the host.

Keywords: Gut microbiota, circadian clock, microbial metabolism, fermentation products

[*] Further information and requests for resources and reagents should be directed to the corresponding authors, Markus Arnoldini (Markus.arnoldini@hest.ethz.ch) and Giorgia Greter (Giorgia.greter@hest.ethz.ch)

Introduction

From regulating our daily sleep-wake cycles to influencing metabolic processes, the circadian clock dominates the rhythm of most life on Earth [1, 2]. The mammalian circadian clock is a fundamental biological process which functions through a tightly regulated network of transcription factors oscillating in positive and negative feedback loops [3, 4, 5, 6, 7]. Light works as a trigger to the hypothalamus, the master pacemaker, which transmits time-of-day signals to the rest of the body to affect fluctuations in physiology and behavior [8, 9]. One of the key behavioral rhythms that is regulated by the circadian clock is food intake [10]. In anticipation of the changing food availability with a change in light, the master pacemaker activates orexigenic pathways and hormone production to increase feeding and activity, which in turn triggers anorexigenic pathways through satiety signals to prepare for fasting and rest [11]. Being synchronous with the 24-hour light-dark cycle increases fitness, and conversely, being asynchronous with the external environment is detrimental to health [12, 13, 14].

Recent research has revealed crucial links between the biological clock, feeding behavior, and the intricate ecosystem of the gut microbiota [15, 16]. The circadian oscillations in food intake in the host result in oscillations in gut microbial metabolism and composition in a circadian pattern [17, 18]. Oscillating immune function in the host also plays a role in shaping the gut microbial ecosystem. For example, immunoglobulin (Ig) A, a key antibody that regulates commensal bacteria community composition, is secreted with a circadian rhythm, and host responses to the invasion of pathogenic bacteria are dependent on the time of day [19, 20, 21].

There is a growing interest in the interplay between the gut microbiota and the host, as it is now thought that not only the host clock regulates the microbiota, but also vice

versa: that the microbiota influences the host circadian rhythm. The microbiota plays a significant role in the amplitude of host clock gene expression oscillations, and is associated with weight gain and reduced longevity in a dysregulated circadian rhythm [22, 23, 24, 25]. In line with this, germ-free (GF) mice, which do not have a microbiota, are less sensitive to the dysregulation of the circadian clock induced by high fat diets [26]. A major way of signaling between the gut microbiota and the host are microbial fermentation products. fermentation products are metabolic byproducts of the microbiota which are used by the host for many metabolic and endocrine functions in the gut-brain axis, as well as for food intake regulation [27, 28, 29]. fermentation product production by the microbiota triggers satiety signaling in the host through various pathways and is thought to play a role in regulating the host circadian rhythm due to the circadian nature of food intake [30, 17]. However, fermentation product concentrations and microbial metabolism are variable due to the higher order interactions that take place in the complex microbial communities in the gut, making it difficult to evaluate mechanistic interactions between the microbiota and the host circadian clock [31].

It has previously been challenging to disentangle the host circadian clock genes and eating patterns from gut microbial metabolism, as metabolic oscillations in the gut microbiota arise from host food intake. In this study, we use an established intervention to acutely increase microbial metabolism in the gut without directly providing calories to the host. This disrupted the normal microbial rhythm that depends on food intake patterns of the host, allowing us to evaluate how microbiota activity regulates host circadian clock gene expression and subsequent eating patterns. We show that microbial metabolism influences host circadian clock gene expression and that this systemically regulates host feeding behavior.

Results

The host circadian rhythm influences microbial metabolic fluctuations

The complexity of the gut microbiota and the higher order interactions in the gut can make it challenging to identify mechanisms by which the microbiota interacts with the host circadian clock [32]. Changes in microbial metabolism are difficult to quantify in a complex microbiota due to crossfeeding and unknown metabolic profiles of the individual species. To overcome this challenge, we colonized germ-free (GF) wild-type C57BL/6 mice with a defined minimal microbiota of three species and bred them for several generations throughout the study. The Easily Accessible Microbiota (EAM) is composed of *Bacteroides thetaiotaomicron* (*B. theta*)*, Eubacterium rectale* (*E. rectale*)*,* and *Escherichia coli* (*E. coli*), and can be used to study bacterial interactions in a well-defined system of relevant microbiota members*.* Bacteroides and Firmicutes have also previously been observed to fluctuate in the microbiota over a 24-hour cycle, coinciding with host feeding [33]. *B. theta* is the most abundant member of the EAM microbiota, but all three species reach high numbers in the gut of colonized mice (Figure 1A). *B. theta, E. rectale,* and *E. coli* are members of the phyla Bacteroidetes, Firmicutes, and Proteobacteria (recently renamed to Bacteroidota, Bacillota, and Pseudomonadota), respectively*,* the three most abundant phyla in the human gut [15, 34]. To investigate the rhythmic fluctuations in the EAM population, we measured the bacterial load in EAM mouse feces every 6 hours over two days. We found no significant rhythmic changes in bacterial population sizes over the course of 2 full cycles (Figure S1A).

Food intake was measured for each mouse using an isolator-housed TSE Phenomaster system [35]. As a readout for microbial metabolism, hydrogen gas

excretion was also measured over time (Figure 1B and Figure S1B). Hydrogen is an abundant byproduct of butyrate production, and *E. rectale* is the only butyrate producer in the EAM, and therefore the dominant hydrogen producer (Figure S1C) [36, 37]. Hydrogen levels fluctuated in a 24-hour period in the EAM mouse, closely following mouse food intake, which provides the non-host-available fibers that the microbiota can metabolize in the gut (Figure 1B). Germ-free mice did not produce measurable levels of hydrogen despite having the same food intake rhythm (Figure 1C).

Lactulose treatment acutely disrupts the diurnal pattern of microbial metabolism

To acutely disrupt the normal diurnal rhythm of microbial metabolism in the gut without directly providing nutrients to the host, we administered lactulose to EAM mice. Lactulose is a disaccharide that cannot be metabolized by mammals, is known to be metabolized by the gut microbiota, and is associated with an increase in hydrogen production and reduced colon pH due to microbial metabolic activity [38, 39, 40]. We administered the lactulose between Zeitgeber times 3 and 4, several hours after the mice had stopped eating and when hydrogen production was decreasing. To control for a potential effect of the oral gavage itself on the microbiota, PBS was administered as a negative control, and all experiments were replicated in GF mice to control for host effects independently of the microbiota.

Mice that were treated with lactulose showed increased hydrogen production two hours after treatment compared to PBS-treated mice, which continued in the normal rhythm of hydrogen production (Figure 2A). There was a significant difference in hydrogen between the mice in the two groups at the endpoint of the experiment, indicating that the microbiota had metabolized the administered lactulose. To

evaluate the duration of the lactulose-dependent change in the diurnal pattern of microbiota metabolism, we repeated the experiment and monitored hydrogen production over the following dark cycle. Hydrogen levels in lactulose treated mice were equal to PBS treated mice by Zeitgeber 15, indicating that the microbiota had metabolized the lactulose and resumed its normal metabolic rhythm, and that our treatment therefore constitutes an acute intervention (Figure 2B). To test whether these results were translatable to a complex microbial community, we performed this experiment in Specific Pathogen Free (SPF) mice. This effect was equally observed in SPF mice, indicating that a complex microbial community also metabolizes lactulose in an acute manner (Figure S2A).

Five hours after the initial lactulose treatment, after the microbiota had metabolized the lactulose, the mice were euthanized, and bacterial population sizes in cecum content were measured to evaluate the effect of lactulose on the EAM microbiota. There was a significant increase in the cecal *E. rectale* population, but no significant change in the numbers of *B. theta* or *E. coli* (Figure 2C). Having observed increased hydrogen production in lactulose-treated mice, we further evaluated the effect of lactulose on microbial metabolism. Microbial metabolism results in an increase in fermentation product production, which should lead to a decrease in pH in the cecum. There was a significant drop in cecum content pH when EAM mice were treated with lactulose, which was associated with an increase in fermentation product concentration in the cecum (Figure 2D and 2E). Lactulose-treated mice had significantly higher concentrations of acetate, butyrate, and succinate, indicating increased metabolic activity of all EAM species, despite the lack of significant increase in *B. theta* and *E. coli* population densities [41, 42]**.** *E. rectale* is the principal butyrate producer in the EAM, while *B. theta* and *E. coli* both produce acetate, and *E. coli* produces succinate (Figure S2B). GF mice that were treated with lactulose

showed a small but significant drop in pH in cecum content, likely due to osmotic effects (Figure 2D). In GF mice, fermentation product concentrations did not increase after lactulose treatment (Figure 2F).

In order to disentangle the osmotic from the metabolic effects of lactulose treatment, we measured the water fraction in feces and cecum content after treatment in EAM mice and GF mice in all experiments. The ratio of the dry fecal weight to the wet fecal weight of GF mice decreased with lactulose treatment, indicating an increase in water content in the feces (Figure S2C). However, the dry to wet feces ratio in EAM mice increased with lactulose treatment, possibly due to the increased microbial biomass from lactulose metabolism, and indicating that the osmotic effect of lactulose treatment was small in these mice. We further controlled for the osmotic effect of lactulose by collecting all the dry feces that were produced by the mice between the treatment and endpoint of the experiment and multiplied the dry weight by the dry/wet weight ratio, thereby calculating the total wet fecal output after treatment (Figure S2D). The osmotic effect of lactulose was weaker than the metabolic effect in EAM mice feces, indicated by the increase in dry weight in feces. When we measured the water content in cecum content, we found no significant difference between treatments in either EAM of GF mice, indicating that the effect of lactulose largely affected fecal water content rather than cecal water content (Figure S2E). Therefore, we concluded that the osmotic effect of lactulose was minimal in the cecum in this study and osmotic effects and subsequent diarrhea in mice are therefore not major contributors to the observed changes in bacterial population sizes and metabolism.

Inducing microbial metabolism acutely increases circadian clock gene expression in small intestinal tissue

To test whether the induction of microbial metabolism affects gene expression driving the host clock, we studied the transcription of several core circadian clock genes in the mouse gastrointestinal tract (Figure 3A). The circadian clock regulation begins with the core clock genes (*CLOCK* and *ARNTL),* which activate transcription of the *Period* and *Cryptochrome* repressor genes [43, 44]. *CLOCK* and *ARNTL* also activate transcription of the *Reverb* and *ROR* genes in a second regulatory loop. Finally, *CLOCK* and *ARNTL* regulate the transcription of *NFIL3* and *DBP* in a third regulatory loop. These genes all function in a transcriptional autoregulatory feedback loop throughout the body.

As described above, EAM mice were treated with lactulose or PBS between zeitgeber time 3-4 and euthanized roughly five hours later. Tissue was harvested from the ileum, cecum, and colon for RNA extraction and RT-PCR. The gene expression of core clock genes was compared between the two treatment groups. When EAM mice were treated with lactulose, there was a significant increase in several core clock genes in the ileum tissue, but no significant difference in gene expression in cecum and colon tissues, where it is presumed that most of the microbial metabolism occurred (Figure 3B and S3A). These differences in expression reflected the fluctuations seen in peripheral tissues in the normal mouse circadian rhythm [45]. To control for the direct effect that lactulose may have on the host, this experiment was also conducted in GF mice. When GF mice were treated with lactulose, there was no significant increase in core clock genes in any of the studied tissues, indicating that microbial metabolism induced changes in the peripheral circadian clock (Figure 3B and S3B). Furthermore, to test whether this effect was translatable to a complex microbiota, this experiment was conducted in SPF mice. When SPF mice were treated with lactulose, there was a significant decrease in

CRY1 expression in the ileum, indicating that the effect of microbial metabolism on SPF clock gene expression was diminished (Figure S3C).

To evaluate the extent of the effect of acute microbial metabolism on clock gene expression, we measured expression in ileum tissue at several time points over 24 hours following lactulose or PBS treatment in EAM mice (Figure 3C). We found that the amplitudes of *CRY1, CRY2,* and to a lesser extent *PER2* expression were significantly increased for several hours after treatment, but that after 24 hours this effect was no longer observed. This finding indicates that the acute effect of lactulose on microbial metabolism also resulted in an acute effect on host clock gene expression.

Inducing microbial metabolism decreases host food intake in following active cycle

We then tested whether increasing host circadian clock gene expression through specific alteration of gut microbial metabolism has further effects on circadian behavior of the host. We measured the rate and total amount of EAM mouse food intake in the dark cycles before and after lactulose treatment. The dark cycle preceding treatment was used to ensure normal feeding behavior for each mouse and provided an undisturbed baseline measurement. Lactulose or PBS treatments were then administered as before at zeitgeber 3-4, and food intake was measured again in the following dark cycle and compared to the baseline food intake in the previous dark cycle. EAM mice treated with lactulose reduced both their food intake rate and total food intake in the following active cycle, while there was no significant reduction in food intake in EAM mice that were treated with PBS (Figure 4A and S4A). We subsequently continued to measure food intake in 5 lactulose-treated mice and 5 PBS-treated mice for a second active cycle, and found that the decrease in

food intake did not persist, indicating an acute effect of microbial metabolism on food intake (Figure S4B).

We repeated this experiment in GF mice and SPF mice and did not find any significant reduction in mice treated with lactulose (Figure 4B and S4C and S4D). The non-significant trend towards lower food intake in lactulose-treated GF mice can potentially be explained by the viscosity of the lactulose solution; viscous solutions given to mice via oral gavage have been shown to decrease food intake [46]. However, the decrease in food intake is small in GF mice compared to EAM mice, indicating that actuation of microbiota metabolism is the dominant cause for this of this effect.

In order to evaluate the mechanism by which microbial metabolism decreases food intake in EAM mice, we assumed that a systemic effect from the small intestine to the rest of the body would require 3 hours. We measured circadian clock gene expression in the EAM hypothalamus and liver 8 hours after lactulose or PBS treatment (Figure 4C). We did not find any significant change in clock gene expression in either of these organs, indicating that the mechanism does not lie in the systemic shift in circadian clock gene expression.

Disruption of food intake patterns is due to systemic effects of microbial metabolic products

Microbial metabolism of lactulose in the mouse takes place largely in the cecum and colon [47]. However, core clock gene expression was most significantly altered in the ileum when mice were administered lactulose. These mice then consumed less food following treatment, implying that the effect of microbial metabolism on the host is systemic and not localized to the point of metabolic processes (Figure 3B and 4A). To test the systemic effect of microbial metabolism on host food intake, EAM mice

were administered a fermentation product mix of succinate, acetate, and butyrate, as these were the fermentation product that were significantly produced by the EAM in the cecum after lactulose treatment (Figure 5A). Orally administered fermentation product are presumed to be taken up by the host in the small intestine, before reaching the cecum [48]. EAM mice reduced their rate of food intake and their total food intake following the treatment of fermentation product, indicating that the effect of the microbiota on host circadian behavior is systemic. When we repeated this experiment in SPF mice, we did not find a significant decrease in food intake following fermentation product treatment (Figure S5A). This is possibly due to uptake efficiency differences in the SPF small intestine compared to the EAM mouse, or due to differences in metabolic signaling processes between these mice.

One potential mechanism by which the microbiota regulates host food intake systemically is by indirect feeding of the host through fermentation products, which can be used for energy harvesting by the host [49]. To evaluate whether the systemic effect of the microbiota reducing host food intake was solely due to the supplemental energy provided by the fermentation product, we estimated the total number of kilocalories that were taken up by the host before and after the treatment with fermentation product, assuming that all fermentation product that were given to the host were used as an energy source (0.19 kcal). We found that mice reduced their food intake by more than the equivalent of 0.19 kcal, showing that the systemic effect goes beyond compensation for the additional energy provided by the microbiota (Figure 5B).

To further evaluate whether this systemic effect of the fermentation product could be observed when they were provided to the host indirectly, we estimated the total maximum number of calories that could be provided to the host by the microbiota after lactulose treatment (Figure 4B). We estimated that the lactulose treatment

provided each mouse with a maximum of 0.52 kcal (Fig. 5C). This maximum value assumes that the energy available to the host from lactulose feeding is equal to the combustion enthalpy of the fed lactulose. This is an overestimation because the host cannot directly metabolize lactulose and gets energy indirectly after the microbiota has extracted significant amounts of energy already. After accounting for the supplementary feeding of the host through fermentation product, we found that EAM mice reduced their food intake following lactulose treatment by even more than 0.52 kcal. This finding indicates that the microbiota has a systemic effect on circadian behavior through a mechanism other than energy homeostasis of the host.

In order to understand the mechanism by which microbial metabolism regulates host food intake, we measured various satiety-associated hormones in EAM, SPF, and GF mice. We measured PYY and GLP-1 concentrations in portal vein plasma, as these are the hormones that known to be associated with gut microbiota changes [50, 51]. We found no significant difference in PYY or GLP-1 concentration in EAM, GF, or SPF mice when treated with lactulose (Figure 5E and 5F). We also measured ghrelin and leptin concentration in heart serum of EAM and GF mice, and found no significant effect of lactulose on their concentrations in EAM mice (Figure S5B and S5C). There was a small but significant increase of ghrelin concentration in lactulose-treated GF mice, potentially due to the osmotic effect of lactulose increasing hunger signaling (Figure S5B).

Discussion

The gut microbiome and host circadian clock are intricately linked, with evidence suggesting that the host circadian clock can influence the gut microbiota and vice versa [52, 33]. In this study, we show that the microbiota regulates host circadian clock gene expression and feeding behavior through metabolic rhythmicity. We first

demonstrated that the EAM gut microbiota oscillates metabolically in a periodic manner which is closely associated with the periodic food intake of the host. Similar rhythmic oscillations in bacterial metabolism have been found independently of microbiota complexities [35, 53, 18]. We disrupted the metabolic rhythmicity of the EAM by providing a nutrient that is available only to the microbiota during the host's fasting period. We observed an acute increase of microbial metabolism following one treatment of lactulose that was comparable to normal production during the host's active state, simulating host food intake for the microbiota [17]. Consequently, we observed an increase of expression of several clock genes in the ileum tissue, some of which persisted for several hours [45].

Most microbial metabolism takes place in the cecum, and interestingly, we found no change in cecum tissue gene expression after treating EAM mice with lactulose. This may indicate a systemic effect of microbial metabolism on the host, rather than a localized one. In fact, a systemic relationship between the gut microbiota and small intestinal epithelial rhythmicity has previously been described as it was found that altering the microbiota through diet causes changes in small intestinal immune function [54, 55]. The systemic effect of the microbiota on the host clock gene expression likely influenced host food intake following the lactulose treatment. We observed an increase in fermentation product concentration in the mouse cecum after administering lactulose to EAM mice, and a subsequent decrease in food intake in the following active cycle. We observed a similar decrease in food intake when we administered a mix of fermentation product directly to the host, indicating that microbial metabolism is in part regulating host feeding behavior. One possible mechanism by which this may occur is through microbial feeding of the host [49]. The microbiota regulates host appetite through energy harvesting of inaccessible fibers: GF mice eat more food in a day than colonized mice to compensate for the reduced

energy extraction in the large intestine that is otherwise provided by the microbiota [35]. By treating EAM mice with lactulose, we assumed that the host would receive energy indirectly from microbial fermentation, and that the host would reduce its food intake in the following dark cycle by the same number of kilocalories. However, after accounting for the energy that the microbiota was providing the host through lactulose metabolism, we still observed a reduction in total energy intake in mice. We observed similar results when we provided the host directly with fermentation product. This finding indicates that providing energy is not the only mechanism by which fermentation product reduce host feeding, and that there is a further mechanism that regulates the host's decrease in total energy harvest.

Surprisingly, when we repeated our experiments in SPF mice we did not observe the same results as in EAM mice. First, we did not measure the same changes in clock gene expression in mice that were treated with lactulose. Furthermore, mice treated with lactulose did not decrease their food intake in the following active cycle. We hypothesized that the microbial composition of the SPF mice resulted in the utilization of fermentation product that were generated after lactulose treatment. However, direct treatment of SPF mice with fermentation product also did not decrease their food intake, indicating that this was not the case. One possible explanation for this difference might be that SPF mice have decreased sensitivity to changes in fermentation products, and that further lactulose doses would induce similar changes in clock gene expression and food intake in SPF mice. Alternatively, there might be a signaling factor in the SPF microbiota that is absent in the EAM, which can block the systemic effect of fermentation products downstream of uptake into the systemic circulation.

fermentation product may have a systemic effect on the host through various mechanisms, and there is an association between fermentation product intake and a

reduction in food intake [56, 51, 57, 58]. Butyrate dietary supplementation in mice decreases food intake and promotes fat oxidation, and acetate supplementation can decrease appetite directly through the blood-brain-barrier [59, 60]. It has also been found that dietary supplements of fermentable carbohydrates which can be broken down by the microbiota result in changes in regulation of satiety hormones which are produced in a circadian manner [61, 50, 62, 63]. However, we did not find any of these hormones to be altered when we treated mice with lactulose, indicating that the systemic effect of microbial metabolism on food intake involves a different mechanism. It has previously been found that mice with gene deletions in the circadian clock lose rhythmicity in food intake and fermentation product concentration in the cecum, indicating the intricate association between the host circadian rhythm and the microbiota [64, 65, 66]. *CRY1* and *CRY2* were upregulated in the ileum for several hours after lactulose treatment, and are known to decrease insulin resistance through the reduction of hepatic gluconeogenesis [67, 68, 69, 70]. Insulin is a hormone that is also associated with satiety, and decreased insulin resistance may have increased satiety in lactulose treated mice [71]. However, there was no significant change in *CRY1/2* in the EAM liver. It is therefore possible that the changes in expression in the ileum resulted in a signaling mechanism to the liver which resulted in acute changes in glucose metabolism and insulin production.

In conclusion, our work demonstrates that the gut microbiota can regulate host food intake through the modulation of the circadian clock. The microbiota breaks down dietary fibers ingested by the host and the metabolic products of microbial metabolism regulate host circadian clock gene expression, which in turn regulates eating behavior. While our results demonstrated an acute effect of diet on the host due to the rapid decoupling of diurnal rhythm and diet, we speculate that the chronic effect of the microbiota on the host through the usual diet of the mouse extends to

factors associated with host circadian rhythm such as endocrine signaling, and that the microbiota plays a significant role in maintaining regular satiety-associated behavior through its metabolic byproducts.

Methods

Lead contact

Further information and requests for resources and reagents should be directed to and will be fulfilled by the lead contact, Markus Arnoldini (Markus.Arnoldini@hest.ethz.ch) or Giorgia Greter (Giorgia.greter@hest.ethz.ch).

Materials availability

All materials are available upon request to the corresponding author.

Data and code availability

All data relevant for generating figures is available in a curated data archive at ETH Zurich under the DOI (http://doi.org/10.3929/ethz-b-000619280). All code used for data analysis and for generating figures is available on Gitlab under the link (https://gitlab.ethz.ch/ggre/circadian_metabolism).

Mice

All strains and resources are listed in the key resources table.

Wild type C57BL/6 mice were maintained on a standard diet at the ETH Phenomics center. Mice were re-derived Germ-free or bred with the EAM microbiota and kept under strict hygienic conditions in breeding isolators. The EAM microbiota was derived using strains *Bacteroides thetaiotaomicron* [72], *Eubacterium rectale* ATCC,

and *Escherichia coli* HS [73]. Specific pathogen free (SPF) mice were bred and housed in individually ventilated cages.All experiments began with 9-15 weeks of age with mixed-sex groups. Mice were fed *ad libitum* for the duration of all experiments and were kept with a dark and light period of 12 hours each. All experiments were approved by the Swiss Kantonal authorities (License ZH120/19 and ZH016/21) according to the legal and ethical requirements.

Metabolic cages

At the start of the experiment, mice were transferred from the breeding isolators to the isolator-housed TSE PhenoMaster® (TSE Systems, Germany) system and were single housed for the duration of the experiment. Mice were acclimated for 4 days after transfer to the metabolic cages. The TSE PhenoMaster® system allows measurements of oxygen, carbon dioxide, and food and water consumption for 160 seconds in 24-minute intervals. Eight metabolic cages were housed in two sterile isolators, and each cage was connected to the system through a HEPA filter. Hydrogen in each cage was measured through a hydrogen sensor (SGP30, Sensirion, Switzerland) which was attached to the TSE Phenomaster® system. Air flow in each cage was set to 0.4 L/min. A two-point calibration of all gases using reference gases was performed within 24 hours of each experiment. The TSE Phenomaster® data and hydrogen data were combined in the data analysis post-experiment.

Mouse experiments

On the fifth day after mouse transfer to the TSE Phenomaster®, mice were treated by oral gavage with either 132mg Lactulose in 100µL PBS, or 100µL PBS. The oral gavage was administered between Zeitgeber 3-4. To measure circadian rhythm changes in the host and changes in the gut, mice were euthanized 5 hours after the

gavage. To measure the changes in clock gene expression over 24 hours, mice were euthanized 8 hours, 12 hours, 18 hours, and 24 hours after the gavage. To measure the effect of lactulose on host food intake, mice were euthanized the day following the treatment or two days following treatment. To measure the effect of fermentation product on host food intake, mice were treated between Zeitgeber 3-4 with 66mg of fermentation product in 100µL of PBS, with a 4:3:3 ratio of sodium succinate, sodium acetate, and sodium butyrate, respectively. Mice which did not eat anything in the 24 hours following oral gavage were excluded from the study.

Bacterial quantification

Mice were euthanized when a peak in hydrogen production was observed following gavage. Wet feces or cecum content were collected from mice and weighed for bacterial quantification. Bacterial DNA was extracted using the DNeasy PowerSoil Pro Kit (Qiagen, Germany). qPCR was performed using the FastStart Universal SYBR Green Master Mix (Roche, Switzerland). Primers for each tested strain were diluted to a final concentration of 1µM. DNA was amplified using a QuantStudio 7 Flex instrument (Applied Biosystems, MA, USA) or a StepOnePlus Real-Time PCR System instrument (Applied Biosystems, MA, USA), with an initial denaturation step of 95°C for 10 minutes, followed by 40 cycles of 95°C for 15 seconds and 60°C for 60 seconds. Bacteria were quantified in each run using a standard curve of known bacterial DNA concentration and corresponding bacterial abundance, which was extracted using the same protocol. Germ-free cecum content and water samples were used to generate a detection limit. For each experiment, a contamination control for *Blautia pseudococcoides* was included in the qPCR, and mice with a C_T lower than 26 in cecum samples were excluded from the study.

Cecal pH measurement

Cecum content was collected in a 2mL Eppendorf tube (Sarstedt, Switzerland) and snap frozen in liquid nitrogen 5 hours after treatment. At the time of measurement, cecum content was thawed and spun down at 1000rpm for 30 seconds to accumulate all content at the bottom of the tube. A pH sensor (Sevencompact S220, Mettler Toledo, Ohio, USA) was completely inserted into the cecum content and pH was measured.

Short chain fatty acid quantification in cecum content

Cecum content was collected in a 2mL Eppendorf tube 5 hours after treatment, snap frozen in liquid nitrogen, and stored at -80°C until further analysis. For UPLC/MS, cecum content was thawed on ice, then homogenized in 70% isopropanol and centrifuged. The supernatant was used for fermentation product quantification using a protocol previously described [74]. A 7-point calibration curve was generated with fermentation product in known concentrations. Calibrators and samples were spiked with a mixture of isotope-labeled internal standards, derivatized to 3-nitrophenylhydrazones, and then quenched with 0.1% formic acid.

An ACQUITY UPLC system (I-Class, Waters, MA, USA) coupled with an Orbitrap Q-Exactive Plus mass spectrometer (Thermo Scientific, San Jose, CA) were used for UPLC/MS analysis. For the fermentation product quantification a Kinetex 2.6 µm XB-C18, 50 × 2.1 mm column (Phenomenex, Torrance, CA, USA) and a flow rate of 250 µL/min was used with a binary mixture of solvent A (water with 0.1% formic acid) and solvent B (acetonitrile with 0.1% formic acid). The gradient starts from 90% of A, then gradually decreases to 75% of A within 6 min and then to 0% of A within 1 min. Then a 0% of A is kept for 1 min and a 90% of A is kept for 1 min to restore the initial solvent ratio. The column was kept at 40°C and the autosampler at 5°C.
Acquired raw data were imported to Skyline (V21.1) and MS2 peaks were integrated. A calibration curve for each compound was built based on the ratio between peak

area of unlabeled and labeled form using a home-built R code. Limit of blank was calculated as mean of the concentration detected in technical blank samples +- 1.645 standard deviation.

Short chain fatty acid quantification in medium

All EAM strains were grown to stationary phase in BHIS medium (reference). After growth, strains were subcultured into 10mL of Epsilon medium and grown overnight (50mM NaCl, 0.02M NH_4Cl, 0.028M K_2HPO_4, 0.072M KH_2PO_4, 50µM $MnCl_2x4H_2O$, 50µM $CoCl_2$, 0.4mM $MgCl_2x6H_2O$, 0.5mM $CaCl_2x2H_2O$, 4µM $FeSO_4x7H_2O$, 20mM $NaHCO_3$, 5mM L-cysteine, 1.2mg/L Hemin, 1mL/L menadione, 2mg/L Folinic acid, 2mG/L Vitamin B12) with 20mM Lactulose as a carbon source. Medium growing *B. theta* and *E. rectale* was supplemented with 1% tryptone, and medium growing *E. coli* was not supplemented with tryptone. 1mL of culture was extracted and filtered in a 0.22µm filter, and fermentation product quantification was performed as previously described [75].

In short, isocratic HPLC was performed in on a Thermo Scientific Ultimate 3000 (Thermo) using 2.5mM H_2SO_4 as mobile phase at a 0.4ml/min flow rate. 20ul of sample was injected, separated over a Phenomenex Rezex RoA organic acid H+ (8%) column kept at 40°C, and compounds were detected using a refractive index detector. Data was recorded for 40min after injection for each sample. Data was analyzed using Python and the package hplc-yp [76].

Dry to wet weight ratio calculation¨

Feces and cecum content were collected 5 hours after treatment and the wet weight was measured. Samples were then lyophilized (Alpha 2-4 LD plus, Martin Christ GmbH, Germany**)** for 48 hours and dry weight was measured. The ratio of dry weight

to wet weight was calculated to estimate the water content in the feces and cecum content after the gavage.

For measuring total fecal output after gavage, the bedding in each cage was replaced at the time of the oral gavage. At the end of the experiment, all fecal pellets were collected and lyophilized. The dry weight of the feces was measured and normalized to the dry to wet weight ratio of each mouse.

RNA extraction

Mouse ileum, cecum, and colon tissues were collected in RNAlater (Thermo Scientific, CA, USA**)** and snap frozen in liquid nitrogen. Samples were stored at -80°C until further analysis. For RNA extractions, samples were thawed on ice and weighed. RNA was extracted using a modified protocol of the Direct-zol RNA kit (Zymo). Samples were mixed with Trizol (Thermo Scientific, CA, USA) and incubated for 5 minutes at room temperature. Samples were then homogenized twice with 0.1mm beads (BioSpec Products, Oklahoma, USA) and 1.0mm silicon carbide beads (BioSpec Products, Oklahoma, USA), for 90 seconds at 30Hz. Further Trizol was mixed with the samples, and centrifuged. Supernatant was mixed with chloroform (Sigma-Aldrich, Switzerland) and centrifuged. Supernatant was then washed in 100% ethanol and centrifuged in collection tubes. RNA was washed in Pre-wash buffer and incubated for 15 minutes at room temperature with 60 units of DNAse. Finally, RNA was washed in Wash buffer and eluted in Nuclease-free water (Invitrogen, Massachusetts, USA).

RNA concentration and quality were measured using a nanodrop machine (ND-1000 Spectrophotometer, Thermo Scientific, CA, USA) and RNA was diluted to a final concentration of 20ng/µL in nuclease-free water. Reverse transcription was done

using the High-Capacity cDNA Reverse Transcription Kit (Applied Biosystems). cDNA was diluted 1:25 in nuclease-free water for qPCR.

Circadian clock gene expression

Host circadian clock gene primers were used to estimate expression using RT-PCR. A housekeeping gene (RPL19) was used for normalization. The RT-PCR was carried out as previously described, and sample extracted RNA was included in a reaction with the housekeeping gene to control for DNA contamination.

Data analysis

Phenomaster quality control

For all measurements, a variable of zeitgeber time (h) was created where 0-12 represents the mouse light phase and 12-24 represents the mouse dark phase. The day number of the experiment was calculated based on the zeitgeber time of the first measurement. Each new day began at zeitgeber time 0, at the start of the light cycle. To account for faulty measurements due to disruptive events and for measurement noise, some datapoints were excluded from the raw dataset. Food intake above 1g and water intake above 1mL in one 24-minute interval for one mouse was considered to have been caused by human disruption and was excluded. Food intake of 0.01g as well as negative food and drink values were considered measurement noise and were excluded. For each mouse, the interquartile range of food and water intake measurements was calculated. Values greater than the 75th percentile + 1.5 times the interquartile range were considered outliers and excluded from the dataset. Potential sources of outlier measurements include food and water loss during human disruption, as well as leaky water bottles. After the data cleanup, mice which had a total daily food intake difference of more than 1g in the two days prior to treatment

were considered not acclimated to the metabolic cages and were excluded from further analysis.

Hydrogen sensor data

The hydrogen sensors attached to the TSE Phenomaster® system measured hydrogen every second, and hydrogen measurements were recorded in a separate file. The median and maximum hydrogen values for each experimental box and reference box measurement were calculated. Median hydrogen values were used for further analysis. If the reference box measurements remained visually constant for the duration of the experiment, the hydrogen data was accepted and merged with the Phenomaster data for further analysis.

Metabolic cage statistical analysis

For estimating daily mouse food intake and hydrogen production, data was extracted from the raw dataset in the two days prior to mouse treatment. For each mouse, the average hydrogen value and food intake measurement per timepoint was calculated. A general additive model was used to fit a curve (using R function mgcv::gam) to these points using the formula y~s(x; bs="cs).

For estimating food intake per day, data was extracted from the beginning of the day prior to mouse treatment to the end of the first dark cycle following treatment, resulting in data from two dark cycles. Cumulative food intake and total food intake were calculated per mouse for each dark cycle, and food intake rate was calculated as the slope of the linear regression of cumulative food intake. A paired T-test was used to compare food intake rate and total food intake for each mouse in the dark cycle prior to treatment and in the dark cycle following treatment.

Energy harvesting estimations

For estimating the indirect caloric intake of the EAM mouse in the lactulose treatment, it was assumed that the EAM metabolized 100% of the lactulose, and that the entirety of the fermentation products of the microbiota were absorbed by the host for caloric feeding. The combustion enthalpy of lactulose was estimated from the combustion enthalpy of lactose (1346 kcal/mol), and the kilocalories from 132mg of lactulose were calculated to be 0.52 per mouse [77]. For estimating the caloric intake of the EAM mouse in the fermentation product treatment, it was assumed that 100% of fermentation product given to the host were used for energy harvesting. The combustion enthalpies and masses provided to the host of acetate (0.21 kcal/mmol, 19.8 mg), butyrate (0.52 kcal/mmol, 19.8 mg), and succinate (0.36 kcal/mmol, 26.4 mg) were used to calculate the maximum possible calories provided to the host (0.19 kcal).

It was assumed that there are 3.94 kilocalories/gram of standard mouse chow [35]. The total caloric intake was calculated per mouse for the dark cycle preceding and following lactulose treatment based on the energy from food intake and indirect feeding from the microbiota and fermentation product treatment. A paired T-test was used to compare caloric intake for each mouse in the dark cycle prior to treatment and in the dark cycle following treatment.

Gene expression

A fluorescence threshold of 0.3 was set for all primers. For data analysis, the delta delta C_T method was used to estimate relative gene expression for each experiment [78]. For samples collected over 24 hours, all gene expression was normalized to untreated mice euthanized at 9AM. For all other samples, gene expression was normalized to the PBS-treated control mice.

For estimating clock gene expression differences in GI tissue and calculating fermentation product concentration in cecum content an unpaired T-test was carried out to compare both groups. To account for false positives in the data analysis, the Benjamini and Hochberg multiple testing correction method was used on both these datasets. For all further comparisons between treatment groups, an unpaired T-test was used to measure differences. All data analysis was carried out using R V4.2.0.

Acknowledgements

We would like to thank Daniel Hoces for providing the base R script which was adapted for analyzing the Phenomaster data. We would further like to thank Sven Nowok and Dominik Bacovcin and the animal caretakers at the EPIC facility at ETHZ for maintaining the mouse lines. We would like to thank Sandra Kaiser, Bidong Nguyen, and Wolf Dietrich-Hardt for providing the Lactulose dosage for this study.

Funding source

This work was supported by the Swiss National Science Foundation (No. 1851228) and was supported as a part of NCCR Microbiomes, a National Centre of Competence in Research, funded by the Swiss National Science Foundation (No. 180575).

Author contributions

G.G., E.S.,and M.A. designed the research. G.G. performed the experiments and data evaluation, and C.M, S.O., A.W.O., E.C.B., and D.K. assisted in the

experiments. J.L. performed the mass spectrometry. G.G. and M.A. wrote the manuscript, in cooperation with all authors.

Declaration of interest

The authors declare no competing interests.

References

[1] J. C. Dunlap, "Molecular Bases for Circadian Clocks," *Cell,* 1999.

[2] I. Robinson and A. B. Reddy, "Molecular mechanisms of the circadian clockwork in mammals," *FEBS Letters,* vol. 588, no. 15, pp. 2477-2483, 8 2014.

[3] C. Dibner, U. Schibler and U. Albrecht, "The mammalian circadian timing system: Organization and coordination of central and peripheral clocks," *Annual Review of Physiology,* vol. 72, pp. 517-549, 3 2009.

[4] N. Gekakis, D. Stakins, H. B. Nguyen, F. C. Davis, L. D. Wilsbacher, D. P. King, J. S. Takahashi and C. J. Weitz, "Role of the CLOCK Protein in the Mammalian Circadian Mechanism," *Science,* 1998.

[5] M. H. Hastings, A. B. Reddy and E. S. Maywood, "A clockwork web: Circadian timing in brain and periphery, in health and disease," *Nature Reviews Neuroscience,* vol. 4, no. 8, pp. 649-661, 2003.

[6] K. Z. M. J. S. S. S. L. P. W. D. R. J. X. M. E. S. H. M. H. R. S. M. Kume, "mCRY1 and mCRY2 Are Essential Components of the Negative Limb of the Circadian Clock Feedback Loop to coordinated circadian outputs from the nucleus, ulti-mately regulating rhythms in physiology and behavior (Welsh et al Circadian clocks also appear to ex," *Cell,* 1999.

[7] L. P. Shearman, S. Sriram, D. R. Weaver, E. S. Maywood, I. I. Chaves, B. Zheng, K. Kume, C. C. Lee, G. T. J. Van Der Horst, M. H. Hastings and S. M. Reppert, "Interacting Molecular Loops in the Mammalian Circadian Clock," *Science,* 2000.

[8] A. Patke, M. W. Young and S. Axelrod, "Molecular mechanisms and physiological importance of circadian rhythms," *Nature Reviews Molecular Cell Biology,* vol. 21, no. 2, pp. 67-84, 2 2020.

[9] M. R. Ralph, R. G. Foster, F. C. Davis and M. Menaker, "Transplanted suprachiasmatic nucleus determines circadian period," *Science,* 1990.

[10] E. Challet, "The circadian regulation of food intake," *Nature Reviews Endocrinology,* vol. 15, no.

7, pp. 393-405, 7 2019.

[11] J. H. Strubbe and G. Van Dijk, "The temporal organization of ingestive behaviour and its interaction with regulation of energy balance," *Neuroscience and Biobehavioral Reviews,* vol. 26, no. 4, pp. 485-498, 6 2002.

[12] L. M. Beaver, B. O. Gvakharia, T. S. Vollintine, D. M. Hege, R. Stanewsky and J. M. Giebultowicz, "Loss of circadian clock function decreases reproductive fitness in males of Drosophila melanogaster," *Proceedings of the National Academy of Sciences of the United States of America,* vol. 99, no. 4, pp. 2134-2139, 2002.

[13] A. B. Reddy and J. S. O'Neill, "Healthy clocks, healthy body, healthy mind," *Trends in Cell Biology,* vol. 20, no. 1, pp. 36-44, 1 2010.

[14] G. C. Yuan, Y. J. Liu, M. F. Dion, M. D. Slack, L. F. Wu, S. J. Altschuler and O. J. Rando, "Molecular biology: Genome-scale identification of nucleosome positions in S. cerevisiae," *Science,* vol. 309, no. 5734, pp. 626-630, 7 2005.

[15] M. A. Mahowald, F. E. Rey, H. Seedorf, P. J. Turnbaugh, R. S. Fulton, A. Wollam, N. Shah, C. Wang, V. Magrini, R. K. Wilson, B. L. Cantarel, P. M. Coutinho, B. Henrissat, L. W. Crock, A. Russell, N. C. Verberkmoes, R. L. Hettich and J. I. Gordon, "Characterizing a model human gut microbiota composed of members of its two dominant bacterial phyla," *PNAS,* 2009.

[16] R. M. Voigt, C. B. Forsyth, S. J. Green, P. A. Engen and A. Keshavarzian, "Circadian Rhythm and the Gut Microbiome," *International Review of Neurobiology,* vol. 131, pp. 193-205, 2016.

[17] Y. Tahara, M. Yamazaki, H. Sukigara, H. Motohashi, H. Sasaki, H. Miyakawa, A. Haraguchi, Y. Ikeda, S. Fukuda and S. Shibata, "Gut Microbiota-Derived Short Chain Fatty Acids Induce Circadian Clock Entrainment in Mouse Peripheral Tissue," *Scientific Reports,* vol. 8, no. 1, 12 2018.

[18] C. A. Thaiss, D. Zeevi, M. Levy, G. Zilberman-Schapira, J. Suez, A. C. Tengeler, L. Abramson, M. N. Katz, T. Korem, N. Zmora, Y. Kuperman, I. Biton, S. Gilad, A. Harmelin, H. Shapiro, Z. Halpern, E. Segal and E. Elinav, "Transkingdom control of microbiota diurnal oscillations promotes metabolic homeostasis," *Cell,* vol. 159, no. 3, pp. 514-529, 10 2014.

[19] M. M. Bellet, E. Deriu, J. Z. Liu, B. Grimaldi, C. Blaschitz, M. Zeller, R. A. Edwards, S. Sahar, S. Dandekar, P. Baldi, M. D. George, M. Raffatellu and P. Sassone-Corsia, "Circadian clock regulates the host response to Salmonella," *Proceedings of the National Academy of Sciences of the United States of America,* vol. 110, no. 24, pp. 9897-9902, 6 2013.

[20] O. Pabst and E. Slack, "IgA and the intestinal microbiota: the importance of being specific," *Mucosal Immunology,* vol. 13, no. 1, pp. 12-21, 1 2020.

[21] H. A. Penny, R. G. Domingues, M. Z. Krauss, F. Melo-Gonzalez, M. A. Lawson, S. Dickson, J. Parkinson, M. Hurry, C. Purse, E. Jegham, C. Godinho-Silva, M. Rendas, H. Veiga-Fernandes, D. A. Bechtold, R. K. Grencis, K. M. Toellner, A. Waisman, J. R. Swann, J. E. Gibbs and M. R. Hepworth, "Rhythmicity of intestinal IgA responses confers oscillatory commensal microbiota mutualism," *Science Immunology,* vol. 7, no. 75, 9 2022.

[22] V. Acosta-Rodríguez, F. Rijo-Ferreira, M. Izumo, P. Xu, M. Wight-Carter, C. B. Green and J. S. Takahashi, "Circadian alignment of early onset caloric restriction promotes longevity in male

C57BL/6J mice," *Science,* 2022.

[23] F. Bishehsari, P. A. Engen, D. Adnan, S. Sarrafi, S. Wilber, M. Shaikh, S. J. Green, A. Naqib, L. B. Giron, M. Abdel-Mohsen and A. Keshavarzian, "Abnormal food timing and predisposition to weight gain: Role of barrier dysfunction and microbiota," *Translational Research,* vol. 231, pp. 113-123, 5 2021.

[24] C. A. Thaiss, M. Levy, T. Korem, L. Dohnalová, H. Shapiro, D. A. Jaitin, E. David, D. R. Winter, M. Gury-BenAri, E. Tatirovsky, T. Tuganbaev, S. Federici, N. Zmora, D. Zeevi, M. Dori-Bachash, M. Pevsner-Fischer, E. Kartvelishvily, A. Brandis, A. Harmelin, O. Shibolet, Z. Halpern, K. Honda, I. Amit, E. Segal and E. Elinav, "Microbiota Diurnal Rhythmicity Programs Host Transcriptome Oscillations," *Cell,* vol. 167, no. 6, pp. 1495-1510.e12, 12 2016.

[25] Y. Wang, Z. Kuang, X. Yu, K. A. Ruhn, M. Kubo and L. V. Hooper, "The intestinal microbiota regulates body composition through NFIL3 and the circadian clock," *Science,* pp. 912-916, 2017.

[26] V. Leone, S. M. Gibbons, K. Martinez, A. L. Hutchison, E. Y. Huang, C. M. Cham, J. F. Pierre, A. F. Heneghan, A. Nadimpalli, N. Hubert, E. Zale, Y. Wang, Y. Huang, B. Theriault, A. R. Dinner, M. W. Musch, K. A. Kudsk, B. J. Prendergast, J. A. Gilbert and E. B. Chang, "Effects of diurnal variation of gut microbes and high-fat feeding on host circadian clock function and metabolism," *Cell Host and Microbe,* vol. 17, no. 5, pp. 681-689, 5 2015.

[27] E. E. Canfora, J. W. Jocken and E. E. Blaak, "Short-chain fatty acids in control of body weight and insulin sensitivity," *Nature Reviews Endocrinology,* vol. 11, no. 10, pp. 577-591, 10 2015.

[28] H. Han, B. Yi, R. Zhong, M. Wang, S. Zhang, J. Ma, Y. Yin, J. Yin, L. Chen and H. Zhang, "From gut microbiota to host appetite: gut microbiota-derived metabolites as key regulators," *Microbiome,* vol. 9, no. 1, 12 2021.

[29] A. Burokas, S. Arboleya, R. D. Moloney, V. L. Peterson, K. Murphy, G. Clarke, C. Stanton, T. G. Dinan and J. F. Cryan, "Targeting the Microbiota-Gut-Brain Axis: Prebiotics Have Anxiolytic and Antidepressant-like Effects and Reverse the Impact of Chronic Stress in Mice," *Biological Psychiatry,* vol. 82, no. 7, pp. 472-487, 10 2017.

[30] S. O. Fetissov, "Role of the gut microbiota in host appetite control: Bacterial growth to animal feeding behaviour," *Nature Reviews Endocrinology,* vol. 13, no. 1, pp. 11-25, 1 2017.

[31] E. Bairey, E. D. Kelsic and R. Kishony, "High-order species interactions shape ecosystem diversity," *Nature Communications,* vol. 7, 8 2016.

[32] A. L. Gould, V. Zhang, L. Lamberti, E. W. Jones, B. Obadia, N. Korasidis, A. Gavryushkin, J. M. Carlson, N. Beerenwinkel and W. B. Ludington, "Microbiome interactions shape host fitness," *PNAS,* 2018.

[33] A. Zarrinpar, A. Chaix, S. Yooseph and S. Panda, "Diet and feeding pattern affect the diurnal dynamics of the gut microbiome," *Cell Metabolism,* vol. 20, no. 6, pp. 1006-1017, 12 2014.

[34] D. Mariat, O. Firmesse, F. Levenez, V. D. Guimar□es, H. Sokol, J. Doré, G. Corthier and J. P. Furet, "The firmicutes/bacteroidetes ratio of the human microbiota changes with age," *BMC Microbiology,* vol. 9, 2009.

[35] D. Hoces, J. Lan, W. Sun, T. Geiser, M. L. Stäubli, E. C. Barazzone, M. Arnoldini, T. D. Challa, M. Klug, A. Kellenberger, S. Nowok, E. Faccin, A. J. Macpherson, B. Stecher, S. Sunagawa, R. Zenobi,

W. D. Hardt, C. Wolfrum and E. Slack, "Metabolic reconstitution of germ-free mice by a gnotobiotic microbiota varies over the circadian cycle," *PLoS Biology,* vol. 20, no. 9, 9 2022.

[36] P. Louis and H. J. Flint, "Diversity, metabolism and microbial ecology of butyrate-producing bacteria from the human large intestine," *FEMS Microbiology Letters,* vol. 294, no. 1, pp. 1-8, 5 2009.

[37] P. Louis and H. J. Flint, "Formation of propionate and butyrate by the human colonic microbiota," *Environmental Microbiology,* vol. 19, no. 1, pp. 29-41, 1 2017.

[38] R. L. Bown, J. A. Gibson, G. E. Sladen, B. Hicks and A. M. Dawson, "Effects of lactulose and other laxatives on ileal and colonic pH as measured by a radiotelemetry device," 1974.

[39] S. Y. Wotzka, M. Kreuzer, L. Maier, M. Zünd, M. Schlumberger, B. Nguyen, M. Fox, D. Pohl, H. Heinrich, G. Rogler, L. Biedermann, M. Scharl, S. Sunagawa, W. D. Hardt and B. Misselwitz, "Microbiota stability in healthy individuals after single-dose lactulose challenge—A randomized controlled study," *PLoS ONE,* vol. 13, no. 10, 10 2018.

[40] Z. Zhang, X. Chen, J. Zhao, C. Tian, X. Wei, H. Li, W. Lin, A. Jiang, R. Feng, J. Yuan and X. Zhao, "Effects of a lactulose-rich diet on fecal microbiome and metabolome in pregnant mice," *Journal of Agricultural and Food Chemistry,* vol. 67, no. 27, pp. 7674-7683, 7 2019.

[41] B. Enjalbert, P. Millard, M. Dinclaux, J. C. Portais and F. Létisse, "Acetate fluxes in Escherichia coli are determined by the thermodynamic control of the Pta-AckA pathway," *Scientific Reports,* vol. 7, 2 2017.

[42] A. A. Salyers, M. O'brien and S. F. Kotarski, "Utilization of Chondroitin Sulfate by Bacteroides thetaiotaomicron Growing in Carbohydrate-Limited Continuous Culture," 1982.

[43] K. H. Cox and J. S. Takahashi, "Circadian clock genes and the transcriptional architecture of the clock mechanism," *Journal of Molecular Endocrinology,* vol. 63, no. 4, pp. R93-R102, 11 2019.

[44] J. S. Takahashi, "Transcriptional architecture of the mammalian circadian clock," *Nature Reviews Genetics,* vol. 18, no. 3, pp. 164-179, 3 2017.

[45] S. Wang, Y. Lin, X. Yuan, F. Li, L. Guo and B. Wu, "REV-ERBα integrates colon clock with experimental colitis through regulation of NF-κB/NLRP3 axis," *Nature Communications,* vol. 9, no. 1, 12 2018.

[46] R. Rasoamanana, P. C. Even, N. Darcel, D. Tomé and G. Fromentin, "Dietary fibers reduce food intake by satiation without conditioned taste aversion in mice," *Physiology and Behavior,* Vols. 110-111, pp. 13-19, 2 2013.

[47] G. Rechkemmer, K. Rönnau and W. V. Engelhardt, "Fermentation of polysaccharides and absorption of short chain fatty acids in the mammalian hindgut," *Comparative Biochemistry and Physiology,* vol. 9, no. 4, pp. 563-568, 1988.

[48] M. G. Schmitt, K. H. Soergel, C. M. Wood and J. J. Steff, "Absorption of Short-Chain Fatty Acids from the Human Ileum," *Digestive Diseases,* 1977.

[49] G. den Besten, K. Lange, R. Havinga, T. H. van Dijk, A. Gerding, K. van Eunen, M. Müller, A. K. Groen, G. J. Hooiveld, B. M. Bakker, D.-J. Reijngoud, d. G. Besten, v. T. Dijk and v. K. Eunen, "Gut-derived short-chain fatty acids are vividly assimilated into host carbohydrates and lipids," *Am J*

Physiol Gastrointest Liver Physiol, vol. 305, pp. 900-910, 2013.

[50] J. Zhou, R. J. Martin, R. T. Tulley, A. M. Raggio, K. L. Mccutcheon, L. Shen, S. C. Danna, S. Tripathy, M. Hegsted, M. J. Keenan and J. Zhou, "Dietary resistant starch upregulates total GLP-1 and PYY in a sustained day-long manner through fermentation in rodents," *Am J Physiol Endocrinol Metab,* vol. 295, pp. 1160-1166, 2008.

[51] E. S. Chambers, A. Viardot, A. Psichas, D. J. Morrison, K. G. Murphy, S. E. Zac-Varghese, K. MacDougall, T. Preston, C. Tedford, G. S. Finlayson, J. E. Blundell, J. D. Bell, E. L. Thomas, S. Mt-Isa, D. Ashby, G. R. Gibson, S. Kolida, W. S. Dhillo, S. R. Bloom, W. Morley, S. Clegg and G. Frost, "Effects of targeted delivery of propionate to the human colon on appetite regulation, body weight maintenance and adiposity in overweight adults," *Gut,* vol. 64, no. 11, pp. 1744-1754, 11 2015.

[52] L. Litichevskiy and C. A. Thaiss, "The Oscillating Gut Microbiome and Its Effects on Host Circadian Biology," *Annual review of Nutrition,* 2022.

[53] X. Liang, F. D. Bushman and G. A. FitzGerald, "Rhythmicity of the intestinal microbiota is regulated by gender and the host circadian clock," *Proceedings of the National Academy of Sciences of the United States of America,* vol. 112, no. 33, pp. 10479-10484, 8 2015.

[54] T. Tuganbaev, U. Mor, S. Bashiardes, T. Liwinski, S. P. Nobs, A. Leshem, M. Dori-Bachash, C. A. Thaiss, E. Y. Pinker, K. Ratiner, L. Adlung, S. Federici, C. Kleimeyer, C. Moresi, T. Yamada, Y. Cohen, X. Zhang, H. Massalha, E. Massasa, Y. Kuperman, P. A. Koni, A. Harmelin, N. Gao, S. Itzkovitz, K. Honda, H. Shapiro and E. Elinav, "Diet Diurnally Regulates Small Intestinal Microbiome-Epithelial-Immune Homeostasis and Enteritis," *Cell,* vol. 182, no. 6, pp. 1441-1459.e21, 9 2020.

[55] N. Arpaia, C. Campbell, X. Fan, S. Dikiy, J. Van Der Veeken, P. Deroos, H. Liu, J. R. Cross, K. Pfeffer, P. J. Coffer and A. Y. Rudensky, "Metabolites produced by commensal bacteria promote peripheral regulatory T-cell generation," *Nature,* vol. 504, no. 7480, pp. 451-455, 2013.

[56] C. L. Adam, S. W. Gratz, D. I. Peinado, L. M. Thomson, K. E. Garden, P. A. Williams, A. J. Richardson and A. W. Ross, "Effects of dietary fibre (pectin) and/or increased protein (casein or pea) on satiety, body weight, adiposity and caecal fermentation in high fat diet-induced obese rats," *PLoS ONE,* vol. 11, no. 5, 5 2016.

[57] J. E. Drew, N. Reichardt, L. M. Williams, C. D. Mayer, A. W. Walker, A. J. Farquharson, S. Kastora, F. Farquharson, G. Milligan, D. J. Morrison, T. Preston, H. J. Flint and P. Louis, "Dietary fibers inhibit obesity in mice, but host responses in the cecum and liver appear unrelated to fiber-specific changes in cecal bacterial taxonomic composition," *Scientific Reports,* vol. 8, no. 1, 12 2018.

[58] J. A. Parnell and R. A. Reimer, "Weight loss during oligofructose supplementation is associated with decreased ghrelin and increased peptide YY in overweight and obese adults," *American Journal of Clinical Nutrition,* vol. 89, no. 6, pp. 1751-1759, 1 2009.

[59] G. Frost, M. L. Sleeth, M. Sahuri-Arisoylu, B. Lizarbe, S. Cerdan, L. Brody, J. Anastasovska, S. Ghourab, M. Hankir, S. Zhang, D. Carling, J. R. Swann, G. Gibson, A. Viardot, D. Morrison, E. L. Thomas and J. D. Bell, "The short-chain fatty acid acetate reduces appetite via a central homeostatic mechanism," *Nature Communications,* vol. 5, 4 2014.

[60] Z. Li, C. X. Yi, S. Katiraei, S. Kooijman, E. Zhou, C. K. Chung, Y. Gao, J. K. Van Den Heuvel, O. C. Meijer, J. F. Berbée, M. Heijink, M. Giera, K. W. Van Dijk, A. K. Groen, P. C. Rensen and Y. Wang, "Butyrate reduces appetite and activates brown adipose tissue via the gut-brain neural circuit," *Gut,* vol. 67, no. 7, pp. 1269-1279, 2018.

[61] P. D. Cani, C. Dewever and N. M. Delzenne, "Inulin-type fructans modulate gastrointestinal peptides involved in appetite regulation (glucagon-like peptide-1 and ghrelin) in rats," *British Journal of Nutrition,* vol. 92, no. 3, pp. 521-526, 9 2004.

[62] M. Gil-Lozano, E. L. Mingomataj, W. K. Wu, S. A. Ridout and P. L. Brubaker, "Circadian secretion of the intestinal hormone GLP-1 by the rodent L cell," *Diabetes,* vol. 63, no. 11, pp. 3674-3685, 11 2014.

[63] J. Qian, C. J. Morris, R. Caputo, M. Garaulet and F. A. Scheer, "Ghrelin is impacted by the endogenous circadian system and by circadian misalignment in humans," *International Journal of Obesity,* vol. 43, no. 8, pp. 1644-1649, 8 2019.

[64] A. Segers, L. Desmet, S. Sun, K. Verbeke, J. Tack and I. Depoortere, "Night-time feeding of Bmal1−/− mice restores SCFA rhythms and their effect on ghrelin," *Journal of Endocrinology,* vol. 245, no. 1, pp. 155-164, 2020.

[65] S. Sen, S. Dumont, D. Sage-Ciocca, S. Reibel, P. de Goede, A. Kalsbeek and E. Challet, "Expression of the clock gene Rev-erbα in the brain controls the circadian organisation of food intake and locomotor activity, but not daily variations of energy metabolism," *Journal of Neuroendocrinology,* vol. 30, no. 1, 1 2018.

[66] S. Yang, A. Liu, A. Weidenhammer, R. C. Cooksey, D. McClain, M. K. Kim, G. Aguilera, E. D. Abel and J. H. Chung, "The role of mPer2 clock gene in glucocorticoid and feeding rhythms," *Endocrinology,* vol. 150, no. 5, pp. 2153-2160, 5 2009.

[67] H. Jang, G. Y. Lee, C. P. Selby, G. Lee, Y. G. Jeon, J. H. Lee, K. K. Y. Cheng, P. Titchenell, M. J. Birnbaum, A. Xu, A. Sancar and J. B. Kim, SREBP1c-CRY1 signalling represses hepatic glucose production by promoting FOXO1 degradation during refeeding, vol. 7, Nature Publishing Group, 2016.

[68] H. S. Dashti, C. E. Smith, Y. C. Lee, L. D. Parnell, C. Q. Lai, D. K. Arnett, J. M. Ordovás and M. Garaulet, CRY1 circadian gene variant interacts with carbohydrate intake for insulin resistance in two independent populations: Mediterranean and North American, vol. 31, Informa Healthcare, 2014, pp. 660-667.

[69] E. E. Zhang, Y. Liu, R. Dentin, P. Y. Pongsawakul, A. C. Liu, T. Hirota, D. A. Nusinow, X. Sun, S. Landais, Y. Kodama, D. A. Brenner, M. Montminy and S. A. Kay, Cryptochrome mediates circadian regulation of cAMP signaling and hepatic gluconeogenesis, vol. 16, 2010, pp. 1152-1156.

[70] M. Hatori and S. Panda, CRY links the circadian clock and CREB-mediated gluconeogenesis., vol. 20, 2010, pp. 1285-1288.

[71] S. C. Woods, T. A. Lutz, N. Geary and W. Langhans, Pancreatic signals controlling food intake; insulin, glucagon and amylin, vol. 361, Royal Society, 2006, pp. 1219-1235.

[72] E. C. Martens, N. M. Koropatkin, T. J. Smith and J. I. Gordon, "Complex glycan catabolism by the human gut microbiota: The bacteroidetes sus-like paradigm," *Journal of Biological Chemistry,*

vol. 284, no. 37, pp. 24673-24677, 9 2009.

[73] M. S. Desai, A. M. Seekatz, N. M. Koropatkin, N. Kamada, C. A. Hickey, M. Wolter, N. A. Pudlo, S. Kitamoto, N. Terrapon, A. Muller, V. B. Young, B. Henrissat, P. Wilmes, T. S. Stappenbeck, G. Núñez and E. C. Martens, "A Dietary Fiber-Deprived Gut Microbiota Degrades the Colonic Mucus Barrier and Enhances Pathogen Susceptibility," *Cell,* vol. 167, no. 5, pp. 1339-1353.e21, 11 2016.

[74] G. Liebisch, J. Ecker, S. Roth, S. Schweizer, V. Öttl, H.-F. Schött, H. Yoon, D. Haller, E. Holler, R. Burkhardt and S. Matysik, "Quantification of Fecal Short Chain Fatty Acids by Liquid Chromatography Tandem Mass Spectrometry—Investigation of Pre-Analytic Stability," *Biomolecules,* vol. 9, no. 4, p. 121, 3 2019.

[75] J. Cremer, M. Arnoldini and T. Hwa, Effect of water flow and chemical environment on microbiota growth and composition in the human colon, vol. 114, National Academy of Sciences, 2017, pp. 6438-6443.

[76] G. Chure and J. Cremer, hplc-py: A Python Package For Rapid Peak Quantification in Complex Chromatograms, 2023.

[77] T. H. Clarke and G. Stegeman, "Heats of Combustion of Some Mono-and Disaccharides," 1939.

[78] K. J. Livak and T. D. Schmittgen, "Analysis of relative gene expression data using real-time quantitative PCR and the 2-ΔΔCT method," *Methods,* vol. 25, no. 4, pp. 402-408, 2001.

[79] S. Brugiroux, M. Beutler, C. Pfann, D. Garzetti, H. J. Ruscheweyh, D. Ring, M. Diehl, S. Herp, Y. Lötscher, S. Hussain, B. Bunk, R. Pukall, D. H. Huson, P. C. Münch, A. C. McHardy, K. D. McCoy, A. J. MacPherson, A. Loy, T. Clavel, D. Berry and B. Stecher, "Genome-guided design of a defined mouse microbiota that confers colonization resistance against Salmonella enterica serovar Typhimurium," *Nature Microbiology,* vol. 2, 11 2016.

[80] A. Steimle, A. De Sciscio, M. Neumann, E. T. Grant, G. V. Pereira, H. Ohno, E. C. Martens and M. S. Desai, "Constructing a gnotobiotic mouse model with a synthetic human gut microbiome to study host–microbe cross talk," *STAR Protocols,* vol. 2, no. 2, 6 2021.

Figures

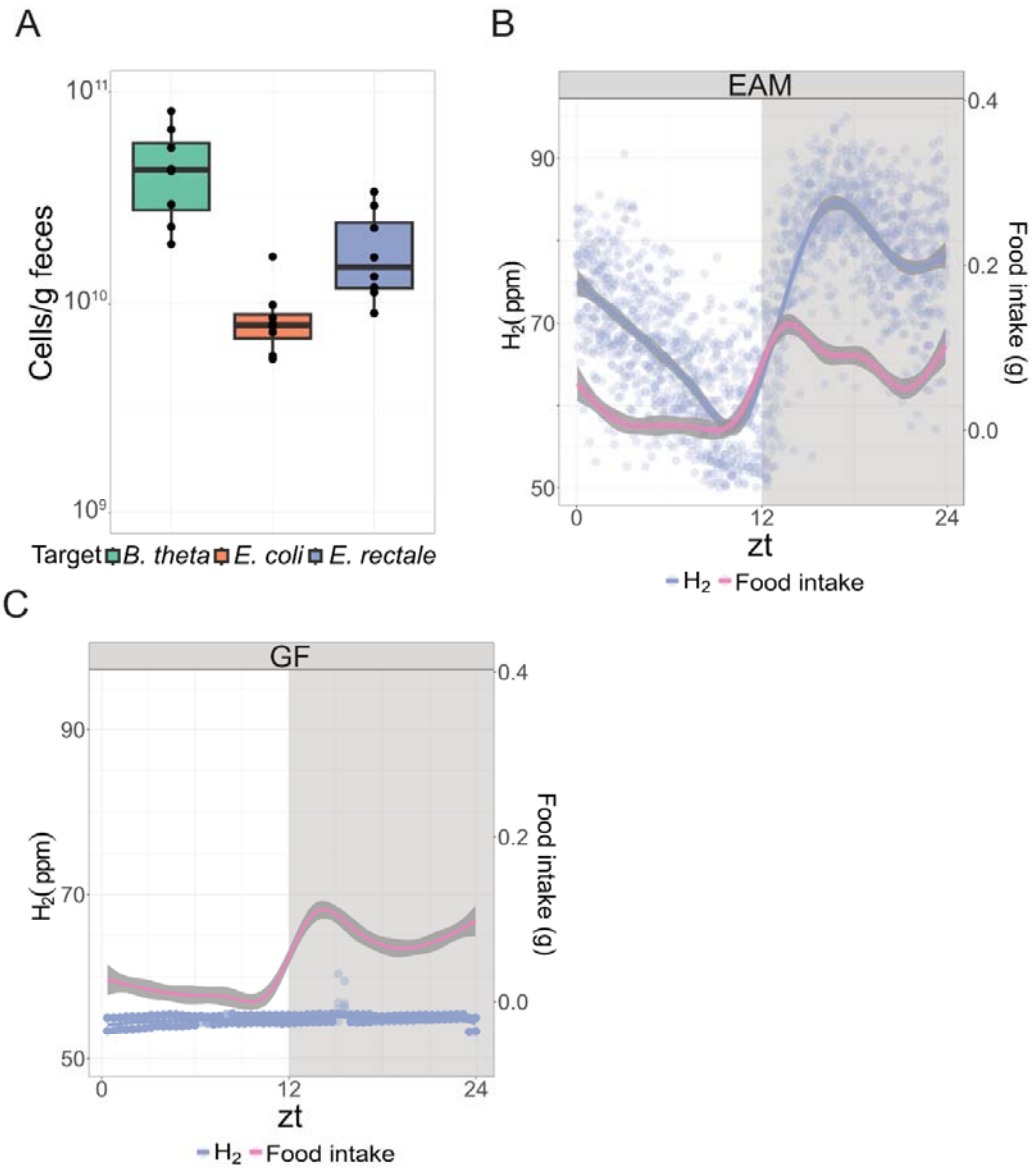

Figure 1: The host circadian rhythm influences microbial cyclical fluctuations. A: Cell counts per grams of feces in the EAM mouse (n=8), calculated by qPCR.**B:** Circadian food intake and hydrogen production of the EAM mouse over two days of measurement, where measurements are taken every 24 minutes (n=16). Curve fit was calculated using formula y~s(x; bs="cs). SE is illustrated with grey shading surrounding line. **C:** Circadian food intake and hydrogen production of the GF mouse (n=8).

630

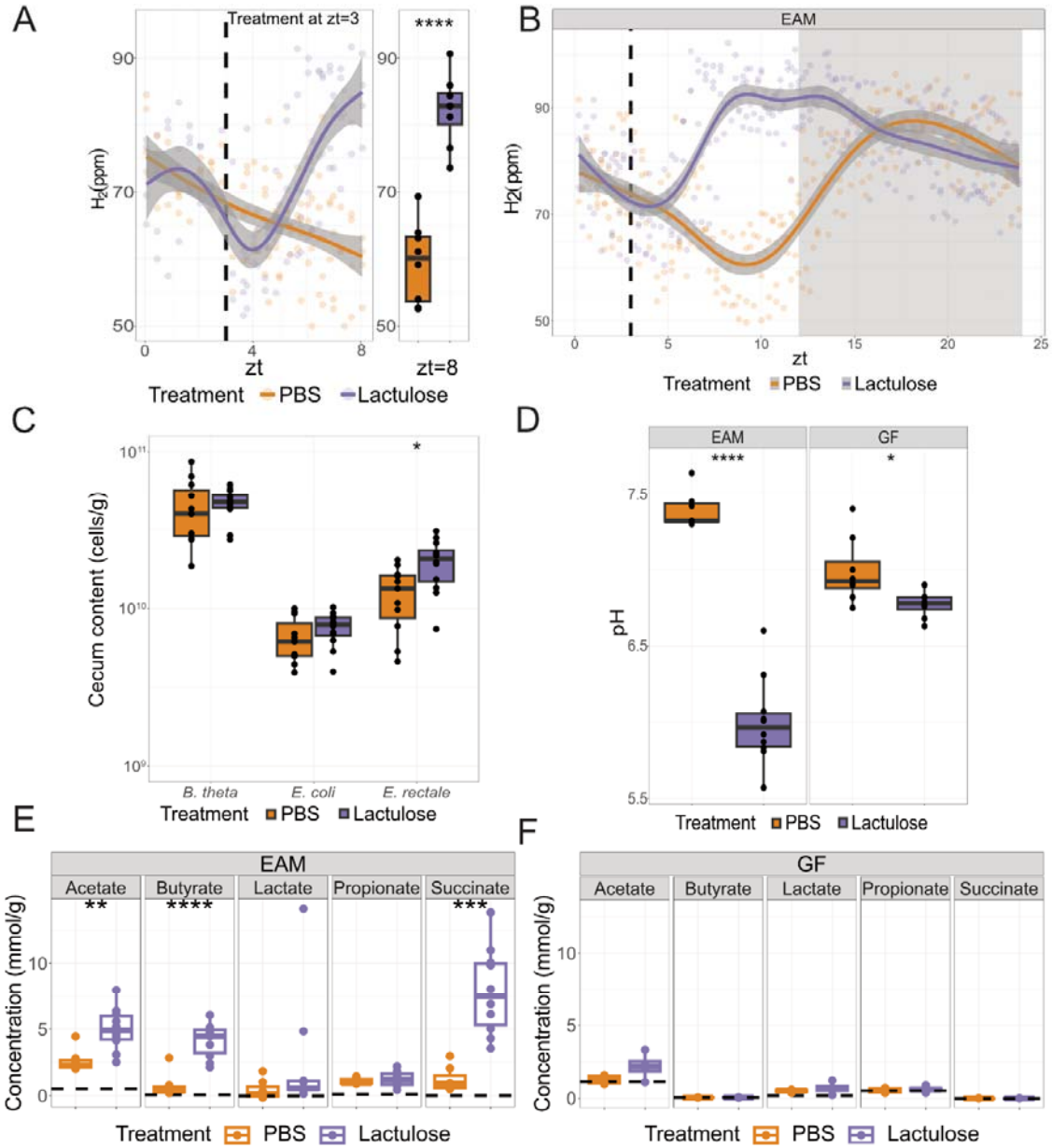

Figure 2: Lactulose disrupts the diurnal rhythm of microbial metabolism. A: Hydrogen production increases after lactulose gavage, but not after PBS gavage (n=16, 8 in each group). Treatment is indicated by a dotted line at zt=3. An unpaired T-test was performed on final hydrogen measurements ($p<0.0001$). **B:** Hydrogen production temporarily increases after lactulose gavage, but not after PBS gavage in EAM mice (n=11, Lactulose=6, PBS=5). Treatment is indicated by a dotted line at zt=3. **C:** Bacterial population after gavage (n=22, lactulose=12, PBS=10). *E. rectale* population increases in lactulose treated mice compared to PBS treated mice ($p<0.05$). **D:** Cecum content pH of EAM (n=17, lactulose=10, PBS=7) and GF (n=16, 8 in each group) mice after treatment. Unpaired T-test revealed a decrease in pH in EAM mice ($p<0.0001$) and GF mice ($p<0.05$). **E:** SCFA concentration in EAM (n=17, lactulose=10, PBS=7) mice after treatment. Unpaired T-test revealed an increase in acetate, butyrate, and succinate concentration after multiple testing correction ("**" = $p<0.01$, "***" = $p<0.001$, "****" = $p<0.0001$). **E:** SCFA concentration in GF (n=8, 4 in each group) mice after treatment. There is no difference in SCFA concentration after treatment.

631

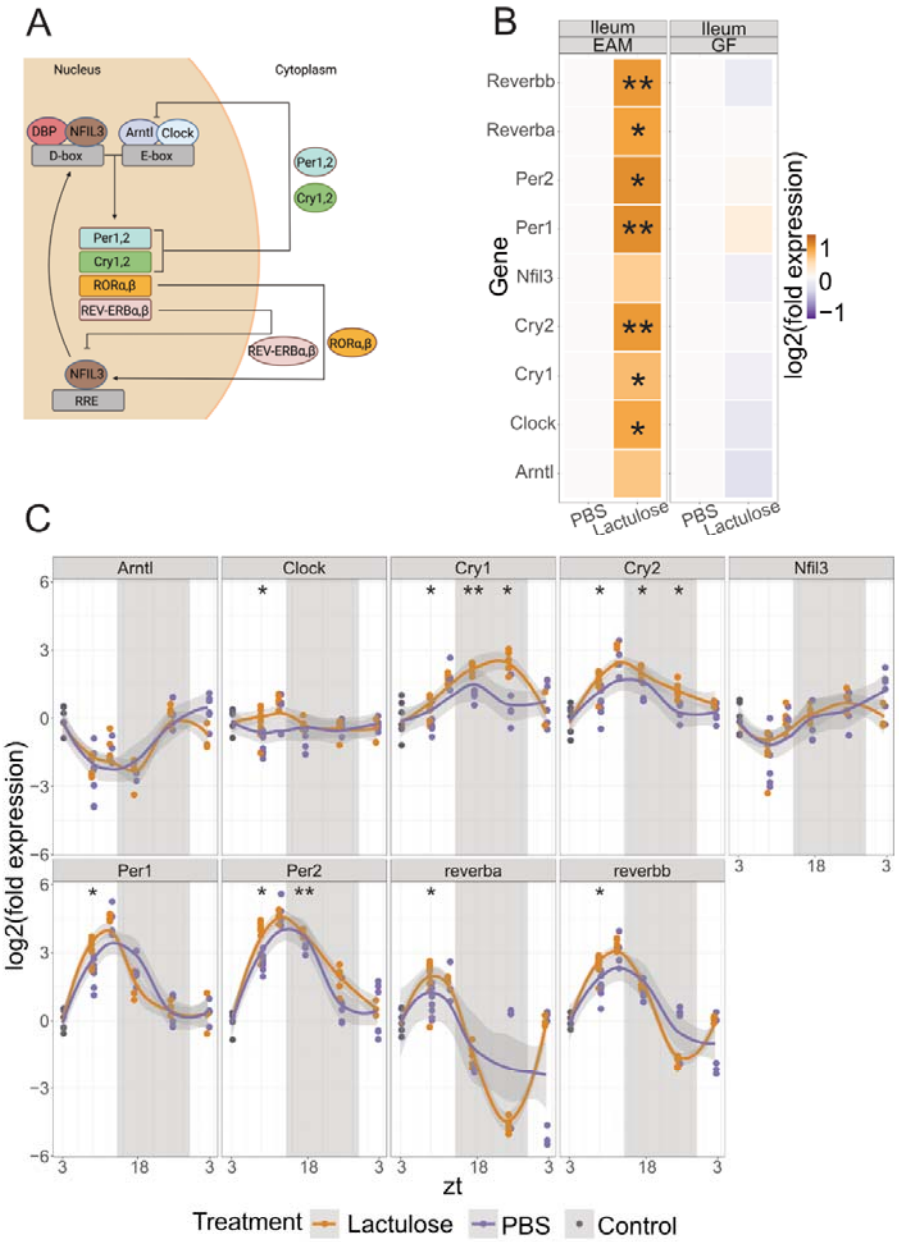

Figure 3: Inducing microbial metabolism acutely alters circadian clock gene expression in small intestinal tissue. A: Schematic of the clock gene network in mice. **B:** Clock gene expression in ileum tissue after EAM mouse treatment (n=17, lactulose=10, PBS=7) and GF mouse treatment (n=16, 8 in each group) measured via RT-PCR. Unpaired T-test revealed increases in EAM gene expression after multiple testing correction ("*" = p<0.05, "**" = p<0.01). **C:** Clock gene expression in EAM mouse ileum tissue over 24 hours after treatment. All gene expression was normalized to samples collected from untreated mice at 9AM (control). Unpaired T-test revealed changes in expression after multiple testing correction ("*"= p<0.05, "**" = p<0.01).

632

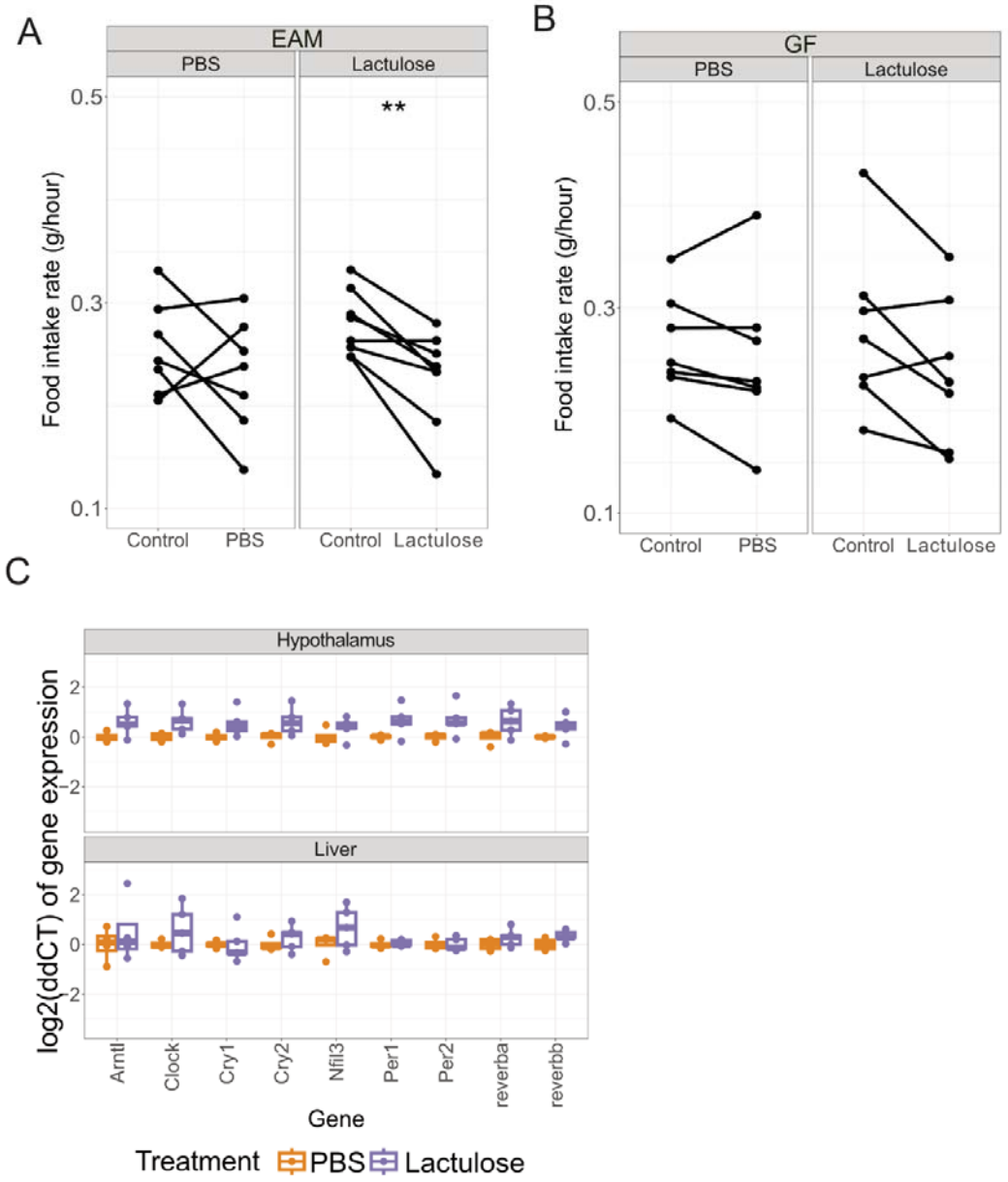

Figure 4: Inducing microbial metabolism decreases host food intake in following active cycle. A: EAM mouse (n=15, lactulose=8, PBS=7) food intake rate in dark phase prior to treatment (control) and following treatment (treatment). Paired T-test displays a reduction in food intake rate after lactulose treatment ($p<0.01$). **B:** GF mouse (n=14, 7 in each group) food intake rate. Paired T-test displays no difference in food intake rate after either treatment. **C:** Clock gene expression in hypothalamus and liver tissues 8 hours after EAM mouse treatment (n=9, lactulose=5, PBS=4) measured via RT-PCR. Unpaired T-test revealed no significant changes in gene expression.

633

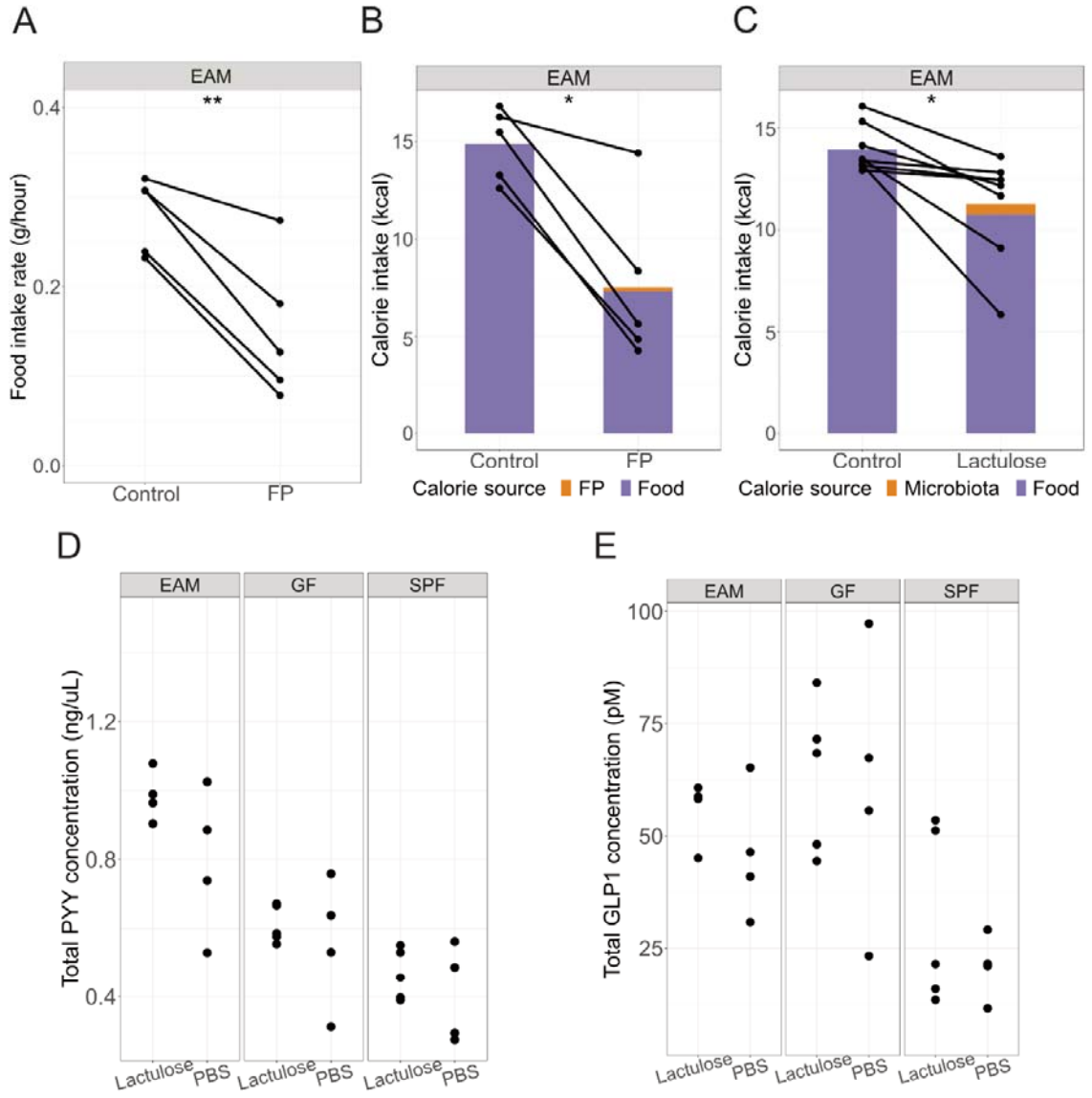

Figure 5: Disruption of circadian food intake patterns is due to systemic effects of microbial metabolic products. A: EAM mouse (n=5) food intake rate in dark phase prior to FP treatment (control) and following treatment (treatment). Paired T-test displays a reduction in food intake rate after FP treatment ($p<0.01$). **B:** EAM mouse total caloric intake after accounting for calories provided by the FP treatment. Paired T-test displays a significant reduction in caloric intake after accounting for calories provided directly by the FP ($p<0.05$). **C:** EAM mouse (data calculated from S4A) total caloric intake after accounting for calories provided by the microbiota after lactulose metabolism. Paired T-test displays a significant reduction in caloric intake after accounting for feeding by the microbiota ($p<0.05$). **D:** Total PYY concentration in portal vein plasma after lactulose or PBS treatment in EAM, GF, and SPF mice. Unpaired T-test revealed no significant differences between groups. **E:** Total GLP-1 concentration in portal vein plasma after lactulose or PBS treatment in EAM, GF, and SPF mice. Unpaired T-test revealed no significant differences between groups.

634

635

Supporting information

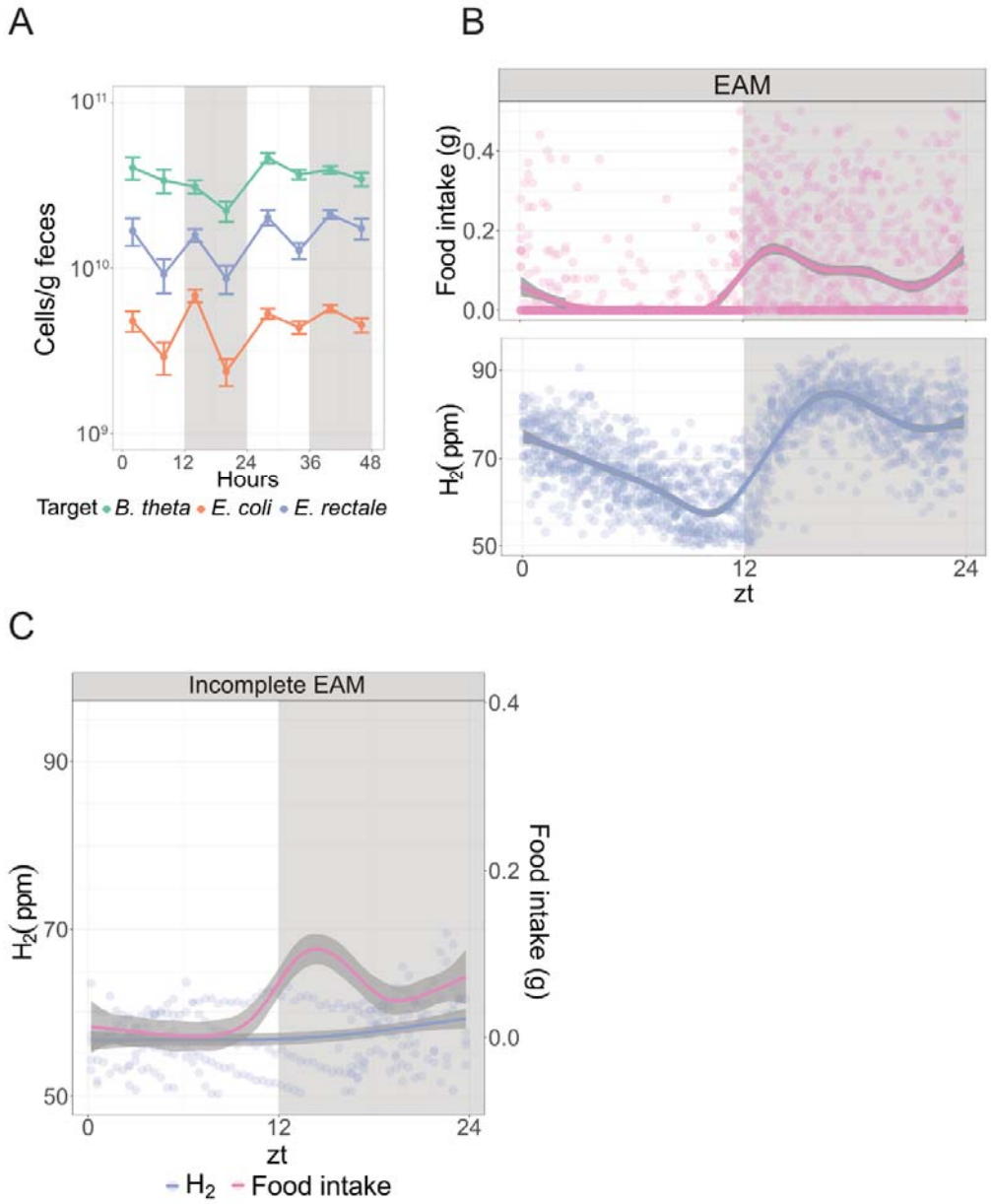

Figure S1: *E. rectale* is the principal hydrogen producer in the EAM. A: Daily fluctuations of EAM strains in mouse feces. Feces were sampled over 2 days (n=8). Shaded regions represent the dark cycle in the animal facility, from zt=12 (6PM) to zt=24 (6AM). **B:**Circadian food intake and hydrogen production of the EAM mouse over two days of measurement, where measurements are taken every 24 minutes (n=16). Curve fit was calculated using formula y~s(x; bs="cs). SE is illustrated with grey shading surrounding line. Shaded regions represent the dark cycle in the animal facility, from zt=12 (6PM) to zt=24 (6AM). **C:** Circadian food intake and hydrogen production of the incomplete EAM (colonized with *B. theta* and *E. coli*) mouse (n=4)

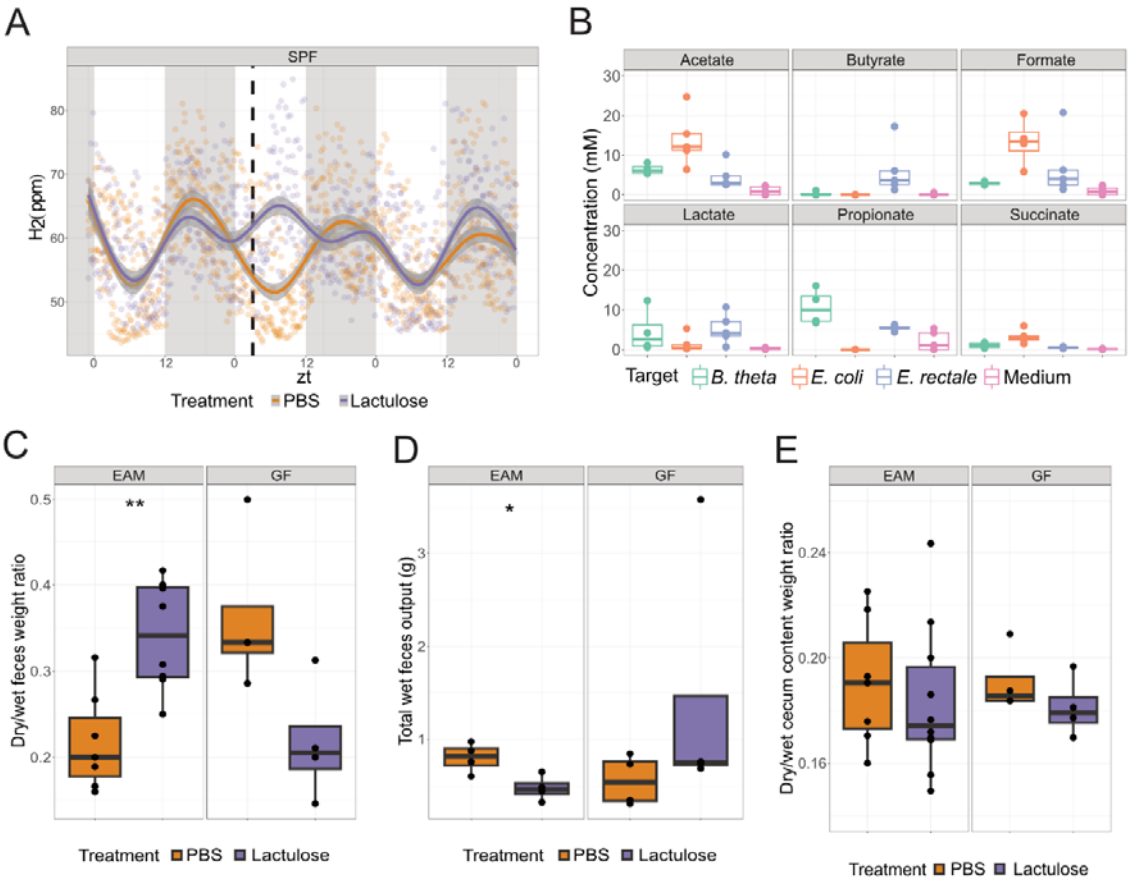

Figure S2: Lactulose disrupts the diurnal rhythm of microbial metabolism. A: Hydrogen production temporarily increases after lactulose gavage, but not after PBS gavage in SPF mice (n=11, Lactulose=5, PBS=6). Treatment is indicated by a dotted line at zt=3.**B:** *in vitro* fermentation product production of EAM when grown on Lactulose. Measurements were taken at stationary phase of growth. **C:**Dry to wet feces ratio in EAM (n=15, lactulose=8, PBS=7) and GF (n=8, 4 in each group) mice. Unpaired T-test shows an increase ($p<0.01$) in the ratio in EAM mice after lactulose treatment. **D:** Total wet feces output after normalizing dry feces weight to mean dry/wet feces ratio in EAM (n=8, 4 in each group) and GF (n=8, 4 in each group) mice. Unpaired T-test shows an increase ($p<0.05$) in the total wet feces output in EAM mice after lactulose treatment. **E:** Dry to wet cecum content ratio in EAM (n=17, lactulose=10, PBS=7).

638

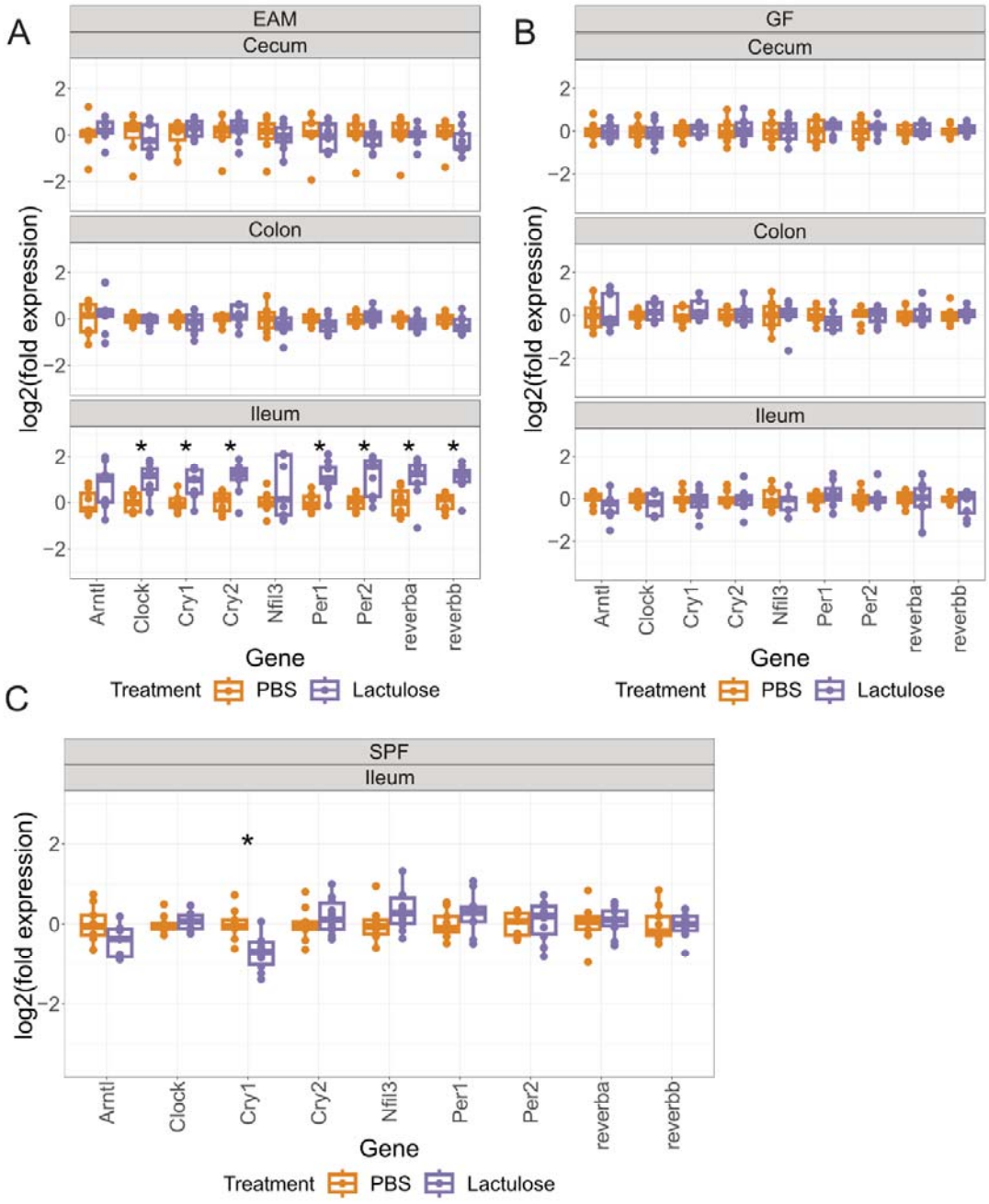

Figure S3: Inducing microbial metabolism acutely alters circadian clock gene expression in small intestinal tissue . A: Clock gene expression in gut tissue after EAM mouse treatment (n=17, lactulose=10, PBS=7) measured via RT-PCR. Unpaired T-test revealed increases in gene expression in the colon and ileum after multiple testing correction ("*" = p<0.05, "**" = p<0.01). **B:** Clock gene expression in gut tissue after GF mouse treatment (n=16, 8 in each group). No significant differences were found in gene expression. **C:** Clock gene expression in ileum tissue after SPF mouse treatment (n=10, 5 in each group). Unpaired T-test revealed decrease in Cry1 expression after multiple testing correction ("*"=p<0.05).

639

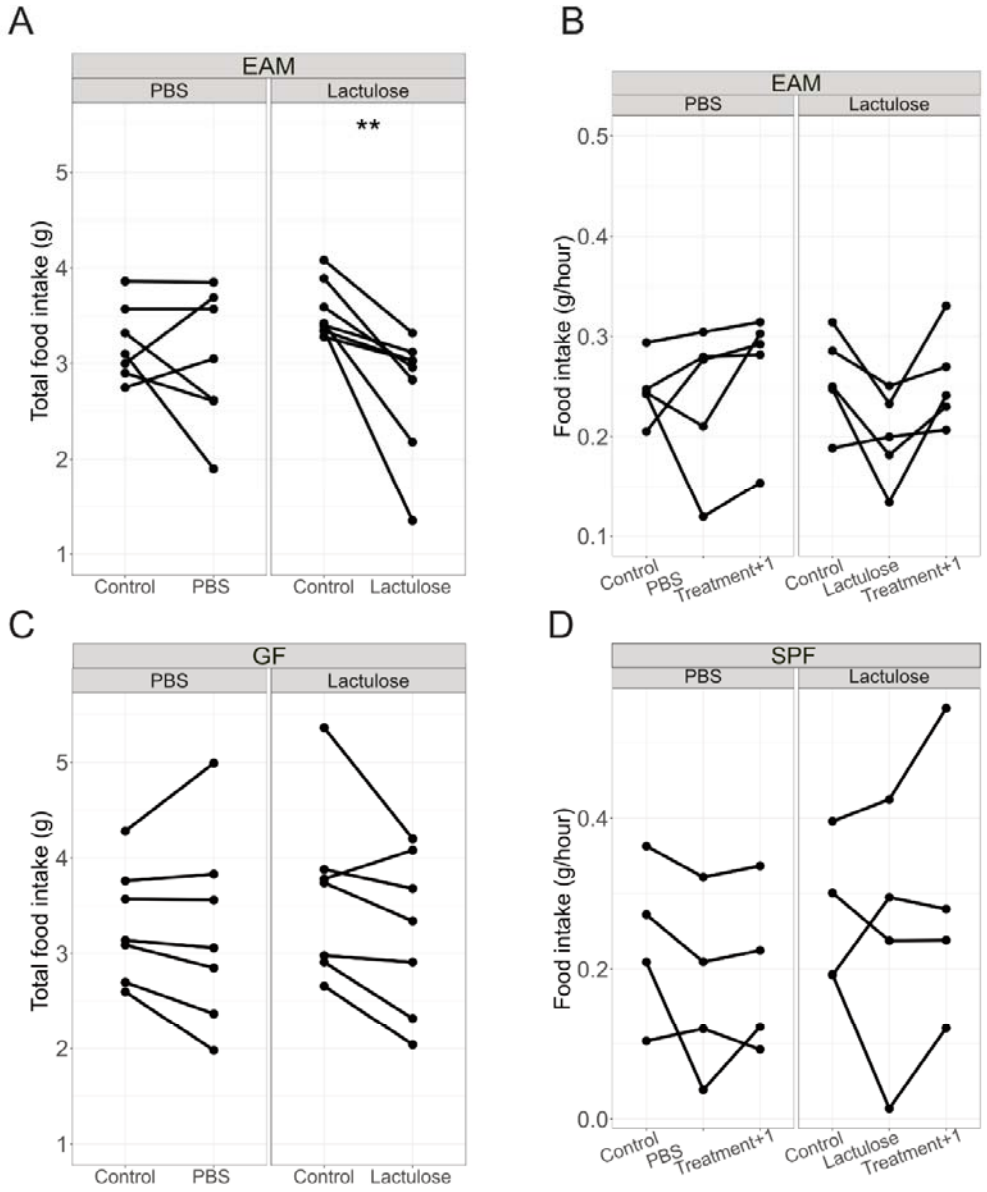

Figure S4: Inducing microbial metabolism decreases host food intake in following active cycle. A: EAM mouse (n=15, lactulose=8, PBS=7) total food intake in dark phase prior to treatment (control) and following treatment (treatment). Paired T-test displays a reduction in food intake rate after lactulose treatment ("**" = p<0.01). **B:**EAM mouse (n=10, lactulose=5, PBS=5) food intake rate in dark phase prior to treatment (control) and two dark phases following treatment (treatment & treatment+1). Anova shows no significant change between the three days. **C:** GF mouse (n=14, 7 in each group) total food intake. Paired T-test displays no difference in food intake rate after either treatment. **D: SPF** mouse (n=8, lactulose=4, PBS=4) food intake rate in dark phase prior to treatment (control) and two dark phases following treatment (treatment & treatment+1). Anova shows no significant change between the three days.

640

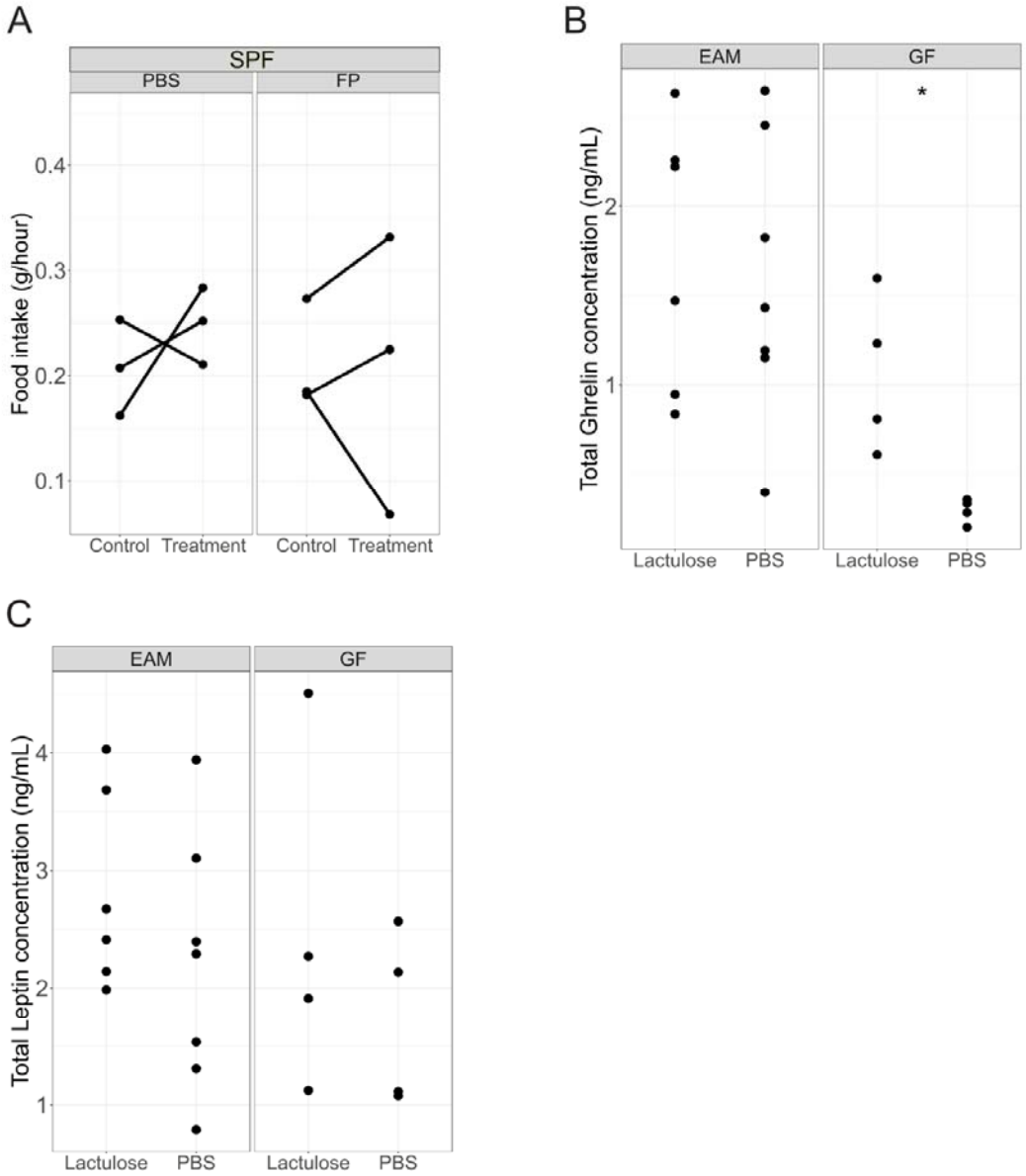

Figure S5: Disruption of circadian food intake patterns is due to systemic effects of microbial metabolic products. A: SPF mouse (n=6, 3 in each group) food intake rate in dark phase prior to PBS or FP treatment (control) and following treatment (treatment). Paired T-test displays no change in food intake rate after FP treatment. **B:** Total ghrelin concentration in heart serum after lactulose or PBS treatment in EAM and GF mice. Unpaired T-test revealed no significant differences between groups in EAM mice, and an increase in ghrelin in GF mice ($p<0.05$). **E:** Total leptin concentration inheart serum after lactulose or PBS treatment in EAM and GF mice. Unpaired T-test revealed no significant differences between groups.

641

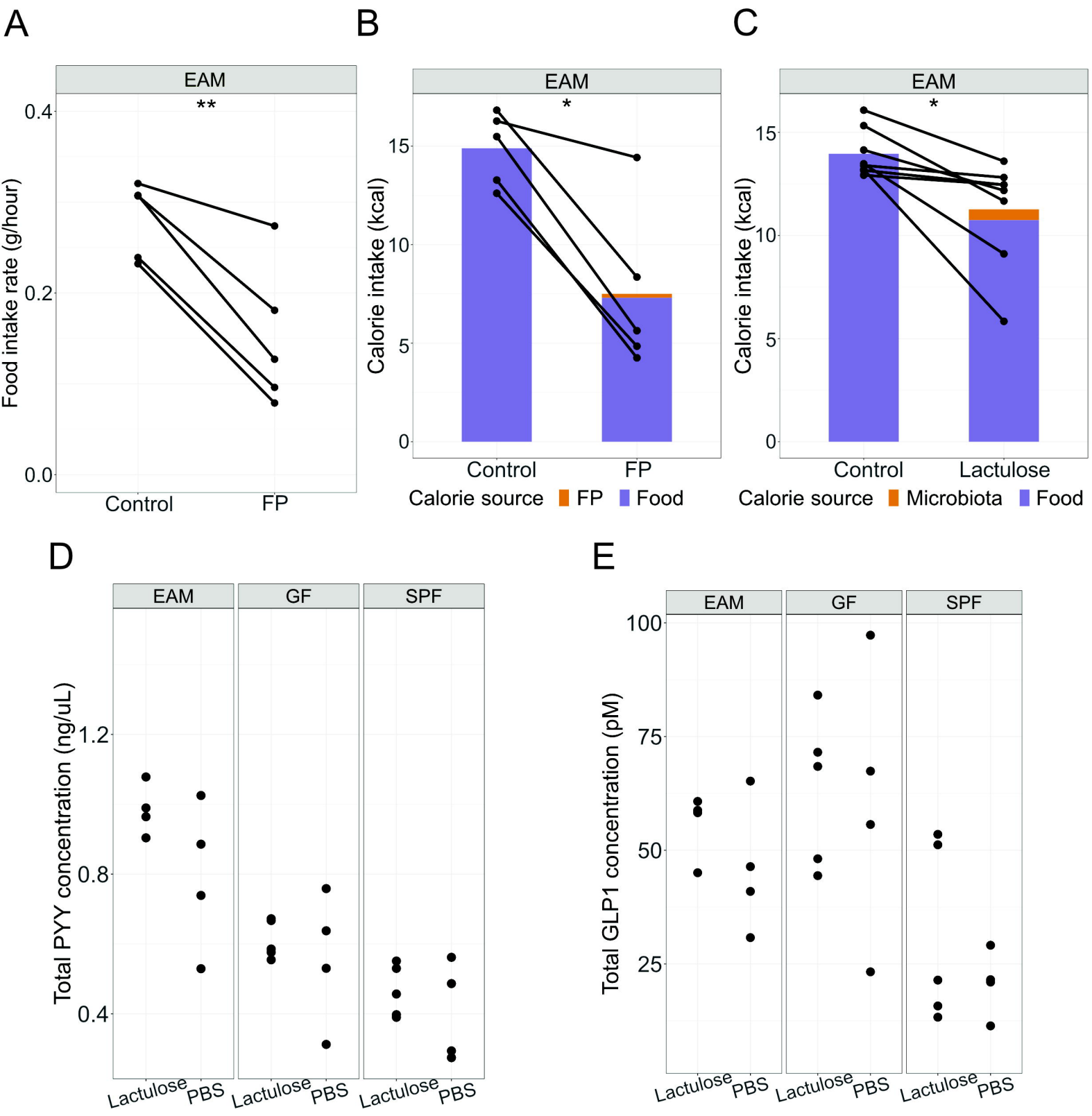

Figure 5: Disruption of circadian food intake patterns is due to systemic effects of microbial metabolic products. A: EAM mouse (n=5) food intake rate in dark phase prior to FP treatment (control) and following treatment (treatment). Paired T-test displays a reduction in food intake rate after FP treatment ($p<0.01$). **B:** EAM mouse total caloric intake after accounting for calories provided by the FP treatment. Paired T-test displays a significant reduction in caloric intake after accounting for calories provided directly by the FP ($p<0.05$). **C:** EAM mouse (data calculated from S4A) total caloric intake after accounting for calories provided by the microbiota after lactulose metabolism. Paired T-test displays a significant reduction in caloric intake after accounting for feeding by the microbiota ($p<0.05$). **D:** Total PYY concentration in portal vein plasma after lactulose or PBS treatment in EAM, GF, and SPF mice. Unpaired T-test revealed no significant differences between groups. **E:** Total GLP-1 concentration in portal vein plasma after lactulose or PBS treatment in EAM, GF, and SPF mice. Unpaired T-test revealed no significant differences between groups.

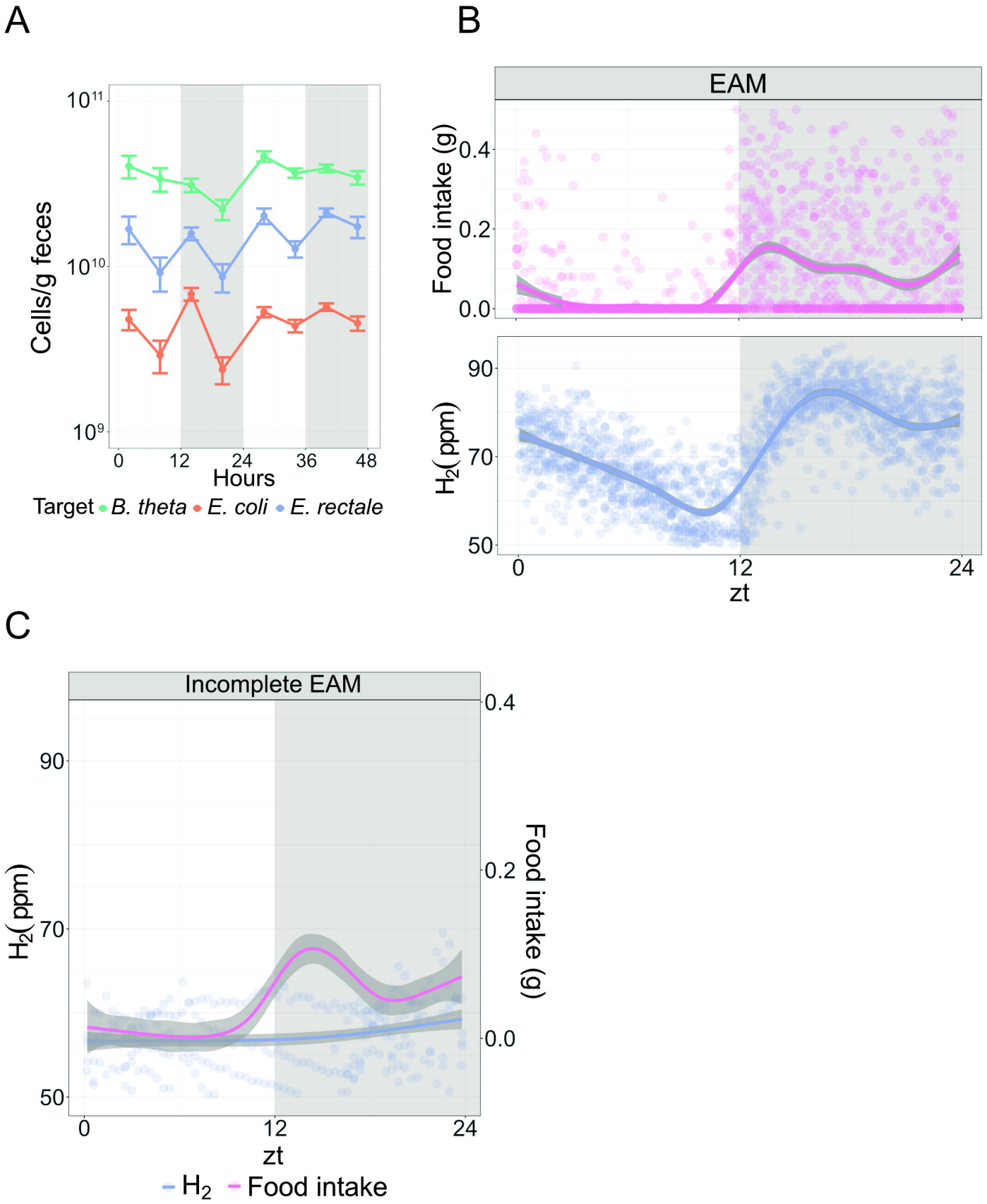

Figure S1: *E. rectale* is the principal hydrogen producer in the EAM. A: Daily fluctuations of EAM strains in mouse feces. Feces were sampled over 2 days (n=8). Shaded regions represent the dark cycle in the animal facility, from zt=12 (6PM) to zt=24 (6AM). **B:**Circadian food intake and hydrogen production of the EAM mouse over two days of measurement, where measurements are taken every 24 minutes (n=16). Curve fit was calculated using formula y~s(x; bs="cs). SE is illustrated with grey shading surrounding line. Shaded regions represent the dark cycle in the animal facility, from zt=12 (6PM) to zt=24 (6AM). **C:** Circadian food intake and hydrogen production of the incomplete EAM (colonized with *B. theta* and *E. coli*) mouse (n=4)

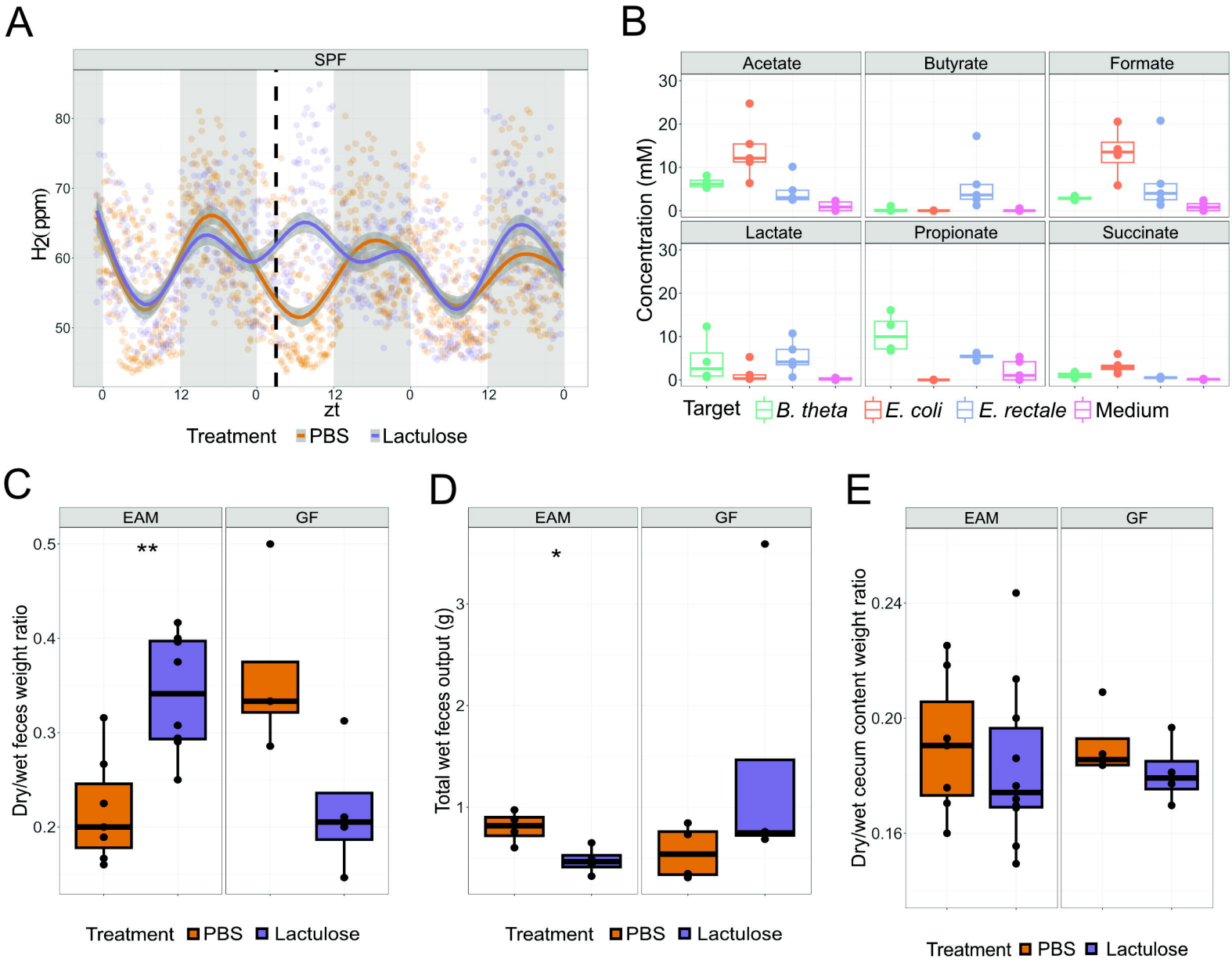

Figure S2: Lactulose disrupts the diurnal rhythm of microbial metabolism. A: Hydrogen production temporarily increases after lactulose gavage, but not after PBS gavage in SPF mice (n=11, Lactulose=5, PBS=6). Treatment is indicated by a dotted line at zt=3.**B:** *in vitro* fermentation product production of EAM when grown on Lactulose. Measurements were taken at stationary phase of growth. **C:**Dry to wet feces ratio in EAM (n=15, lactulose=8, PBS=7) and GF (n=8, 4 in each group) mice. Unpaired T-test shows an increase ($p<0.01$) in the ratio in EAM mice after lactulose treatment. **D:** Total wet feces output after normalizing dry feces weight to mean dry/wet feces ratio in EAM (n=8, 4 in each group) and GF (n=8, 4 in each group) mice. Unpaired T-test shows an increase ($p<0.05$) in the total wet feces output in EAM mice after lactulose treatment. **E:** Dry to wet cecum content ratio in EAM (n=17, lactulose=10, PBS=7).

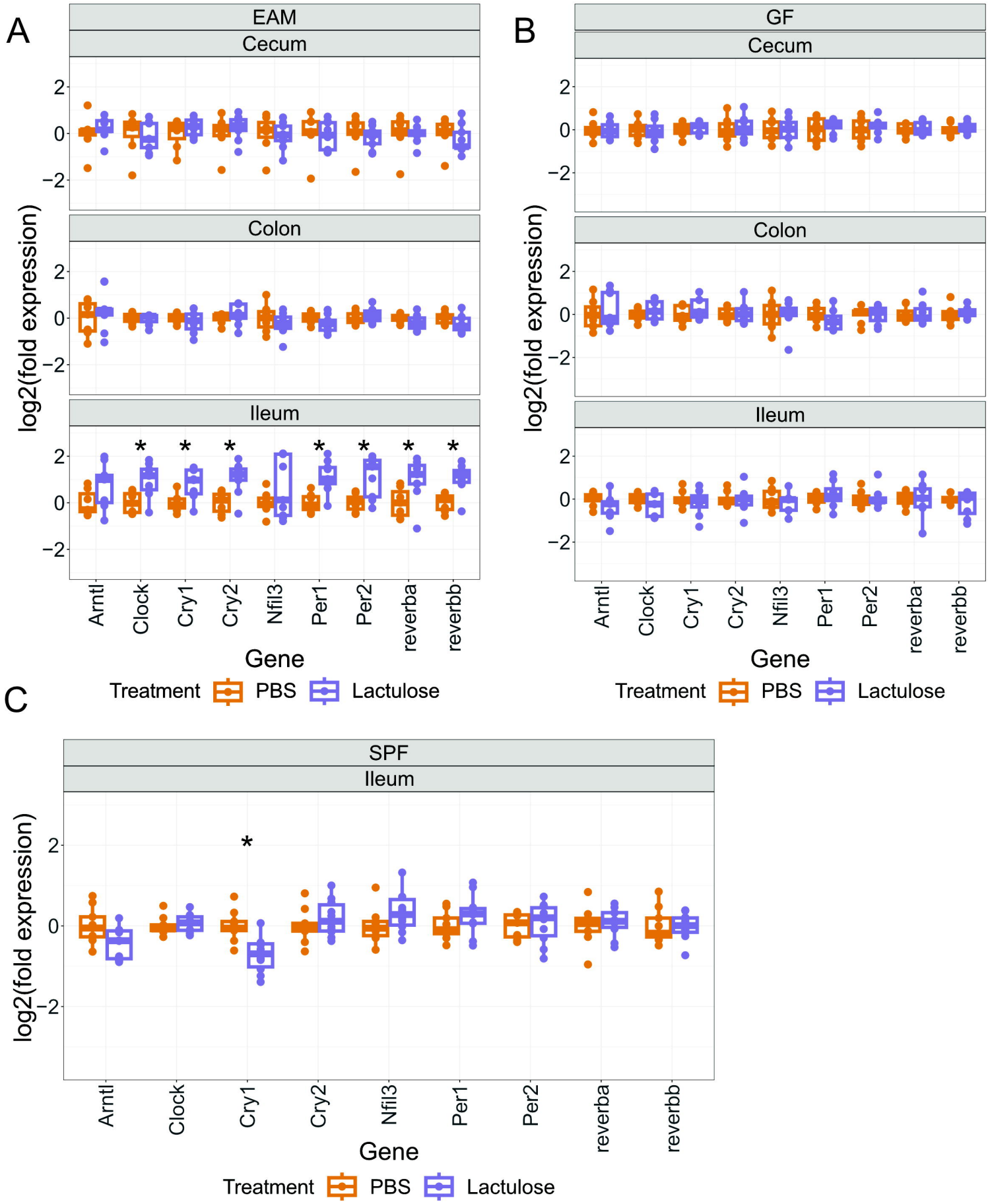

Figure S3: Inducing microbial metabolism acutely alters circadian clock gene expression in small intestinal tissue . A: Clock gene expression in gut tissue after EAM mouse treatment (n=17, lactulose=10, PBS=7) measured via RT-PCR. Unpaired T-test revealed increases in gene expression in the colon and ileum after multiple testing correction ("*" = p<0.05, "**" = p<0.01). **B:** Clock gene expression in gut tissue after GF mouse treatment (n=16, 8 in each group). No significant differences were found in gene expression. **C:** Clock gene expression in ileum tissue after SPF mouse treatment (n=10, 5 in each group). Unpaired T-test revealed decrease in Cry1 expression after multiple testing correction ("*"=p<0.05).

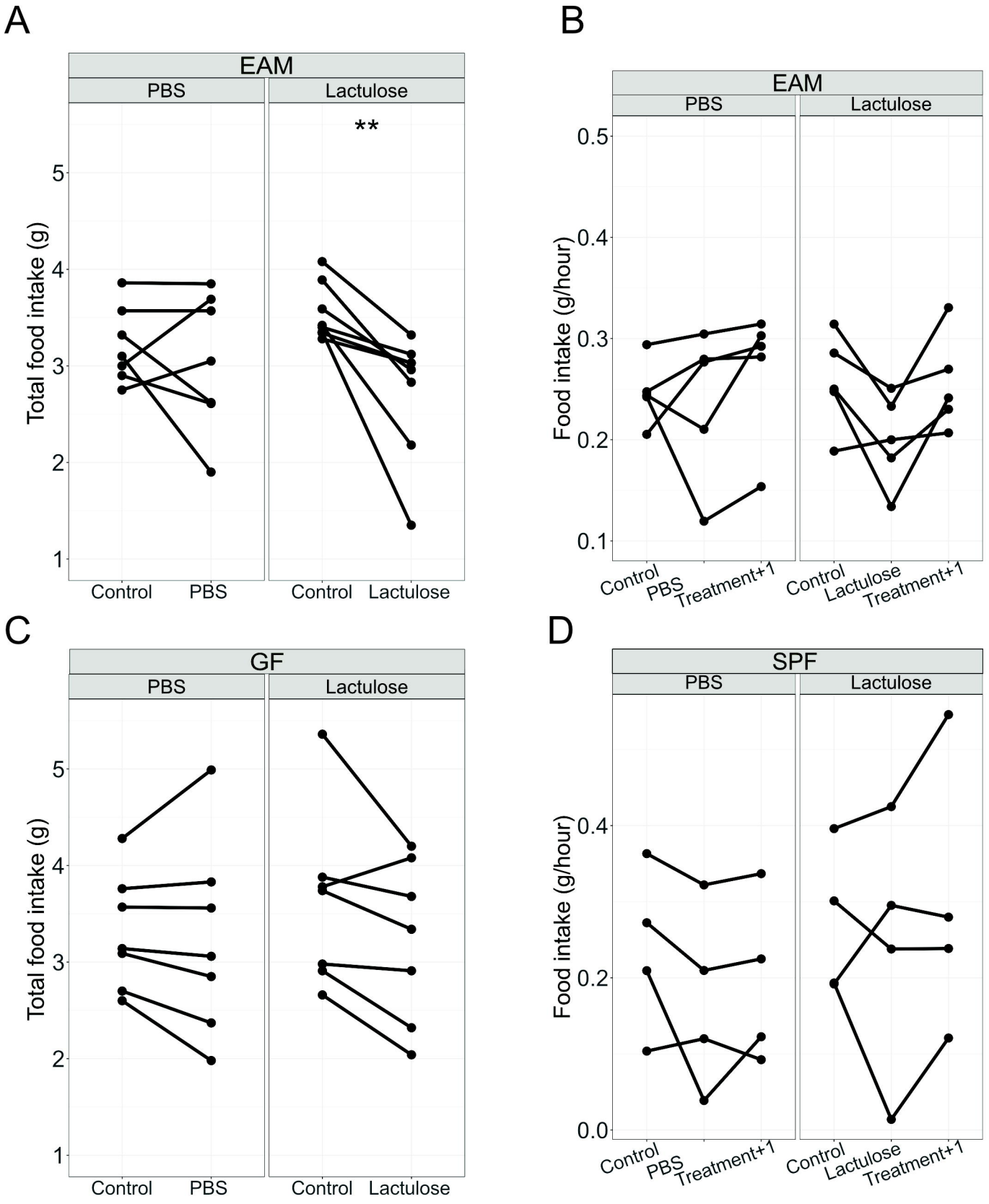

Figure S4: Inducing microbial metabolism decreases host food intake in following active cycle. A: EAM mouse (n=15, lactulose=8, PBS=7) total food intake in dark phase prior to treatment (control) and following treatment (treatment). Paired T-test displays a reduction in food intake rate after lactulose treatment ("**" = p<0.01). **B:**EAM mouse (n=10, lactulose=5, PBS=5) food intake rate in dark phase prior to treatment (control) and two dark phases following treatment (treatment & treatment+1). Anova shows no significant change between the three days. **C:** GF mouse (n=14, 7 in each group) total food intake. Paired T-test displays no difference in food intake rate after either treatment. **D: SPF** mouse (n=8, lactulose=4, PBS=4) food intake rate in dark phase prior to treatment (control) and two dark phases following treatment (treatment & treatment+1). Anova shows no significant change between the three days.

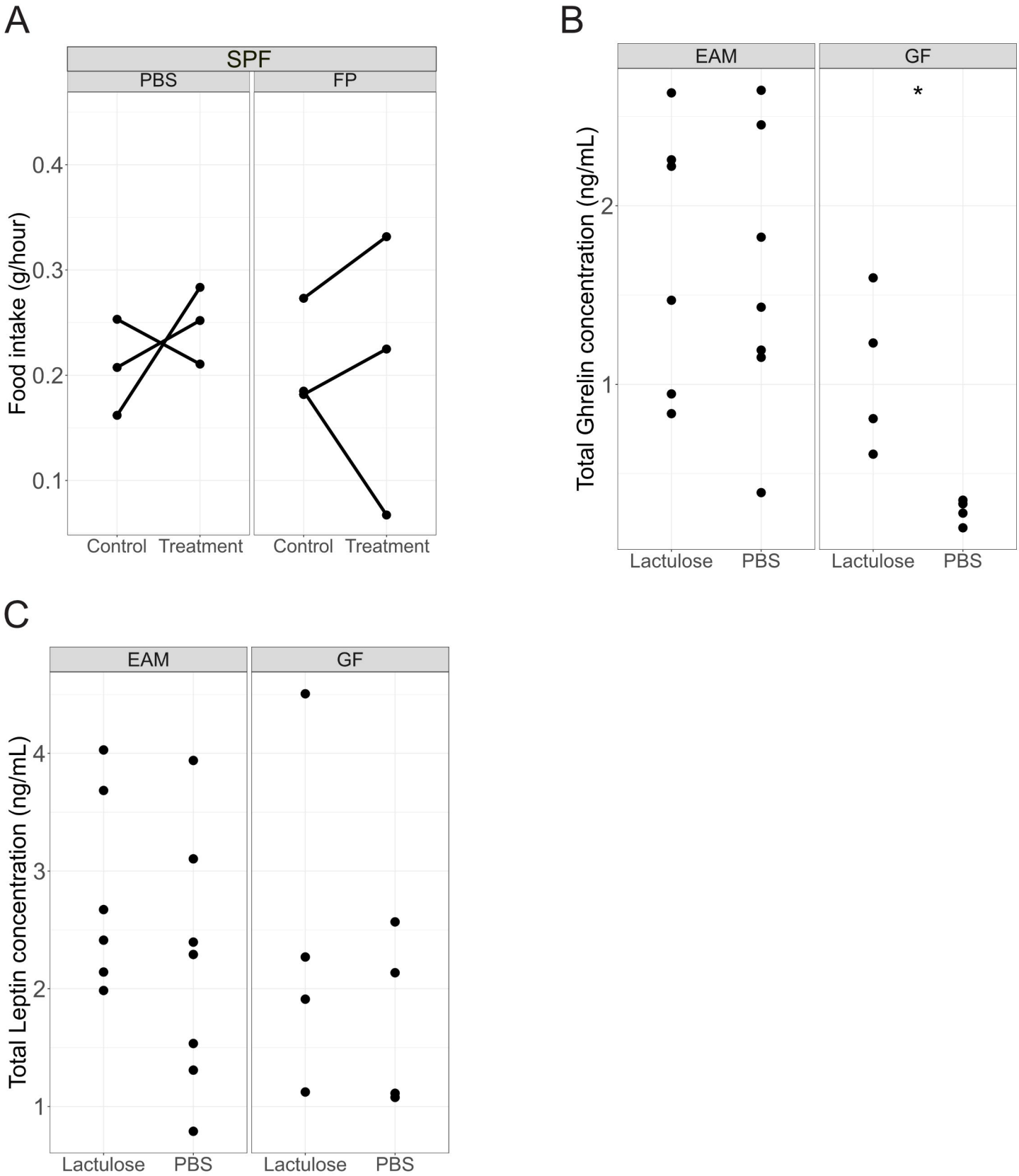

Figure S5: Disruption of circadian food intake patterns is due to systemic effects of microbial metabolic products. A: SPF mouse (n=6, 3 in each group) food intake rate in dark phase prior to PBS or FP treatment (control) and following treatment (treatment). Paired T-test displays no change in food intake rate after FP treatment. **B:** Total ghrelin concentration in heart serum after lactulose or PBS treatment in EAM and GF mice. Unpaired T-test revealed no significant differences between groups in EAM mice, and an increase in ghrelin in GF mice ($p<0.05$). **E:** Total leptin concentration inheart serum after lactulose or PBS treatment in EAM and GF mice. Unpaired T-test revealed no significant differences between groups.

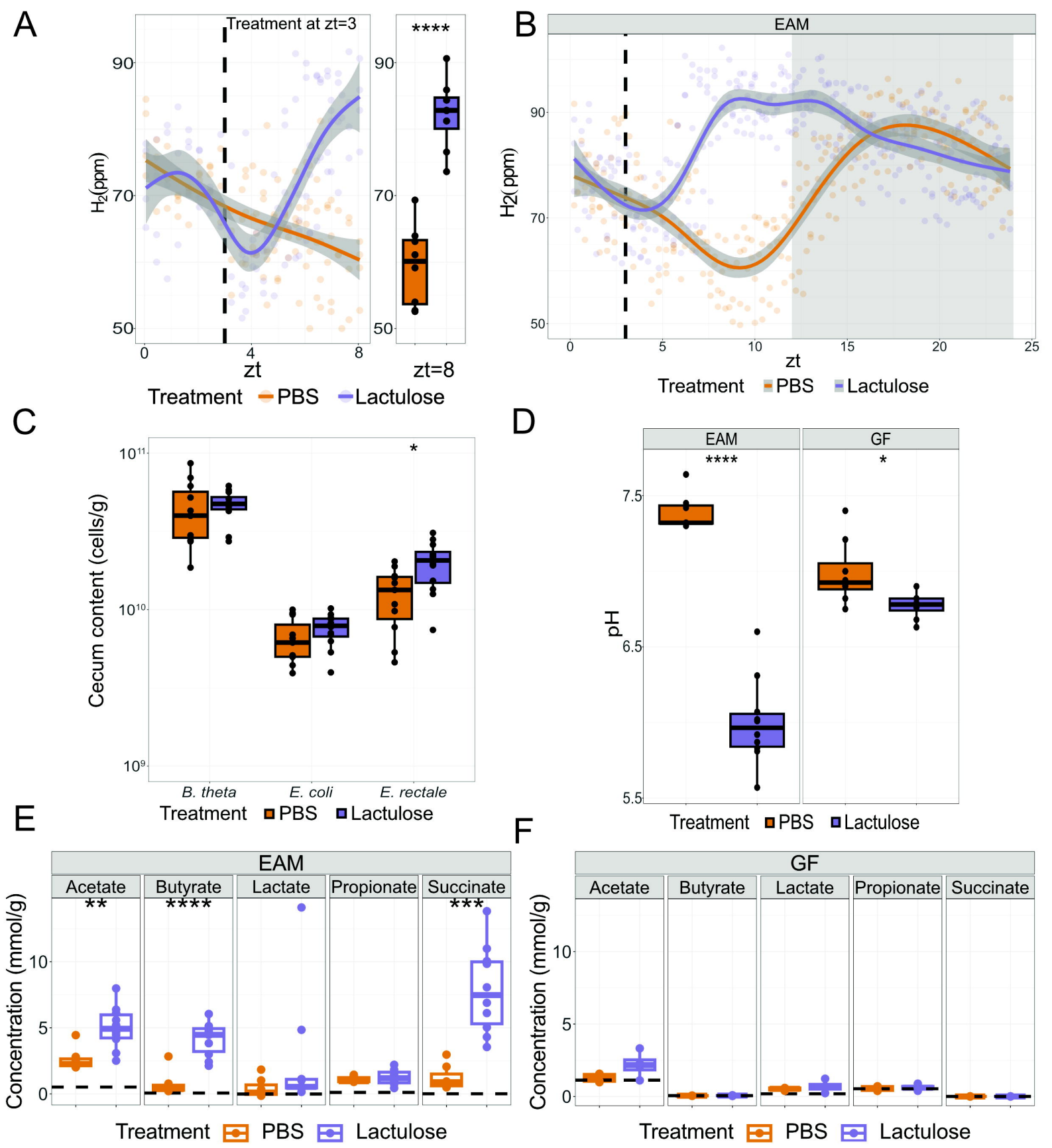

Figure 2: Lactulose disrupts the diurnal rhythm of microbial metabolism. A: Hydrogen production increases after lactulose gavage, but not after PBS gavage (n=16, 8 in each group). Treatment is indicated by a dotted line at zt=3. An unpaired T-test was performed on final hydrogen measurements ($p<0.0001$). **B:** Hydrogen production temporarily increases after lactulose gavage, but not after PBS gavage in EAM mice (n=11, Lactulose=6, PBS=5). Treatment is indicated by a dotted line at zt=3. **C:** Bacterial population after gavage (n=22, lactulose=12, PBS=10). *E. rectale* population increases in lactulose treated mice compared to PBS treated mice ($p<0.05$). **D:** Cecum content pH of EAM (n=17, lactulose=10, PBS=7) and GF (n=16, 8 in each group) mice after treatment. Unpaired T-test revealed a decrease in pH in EAM mice ($p<0.0001$) and GF mice ($p<0.05$). **E:** SCFA concentration in EAM (n=17, lactulose=10, PBS=7) mice after treatment. Unpaired T-test revealed an increase in acetate, butyrate, and succinate concentration after multiple testing correction ("**" = $p<0.01$, "***" = $p<0.001$, "****" = $p<0.0001$). **E:** SCFA concentration in GF (n=8, 4 in each group) mice after treatment. There is no difference in SCFA concentration after treatment.

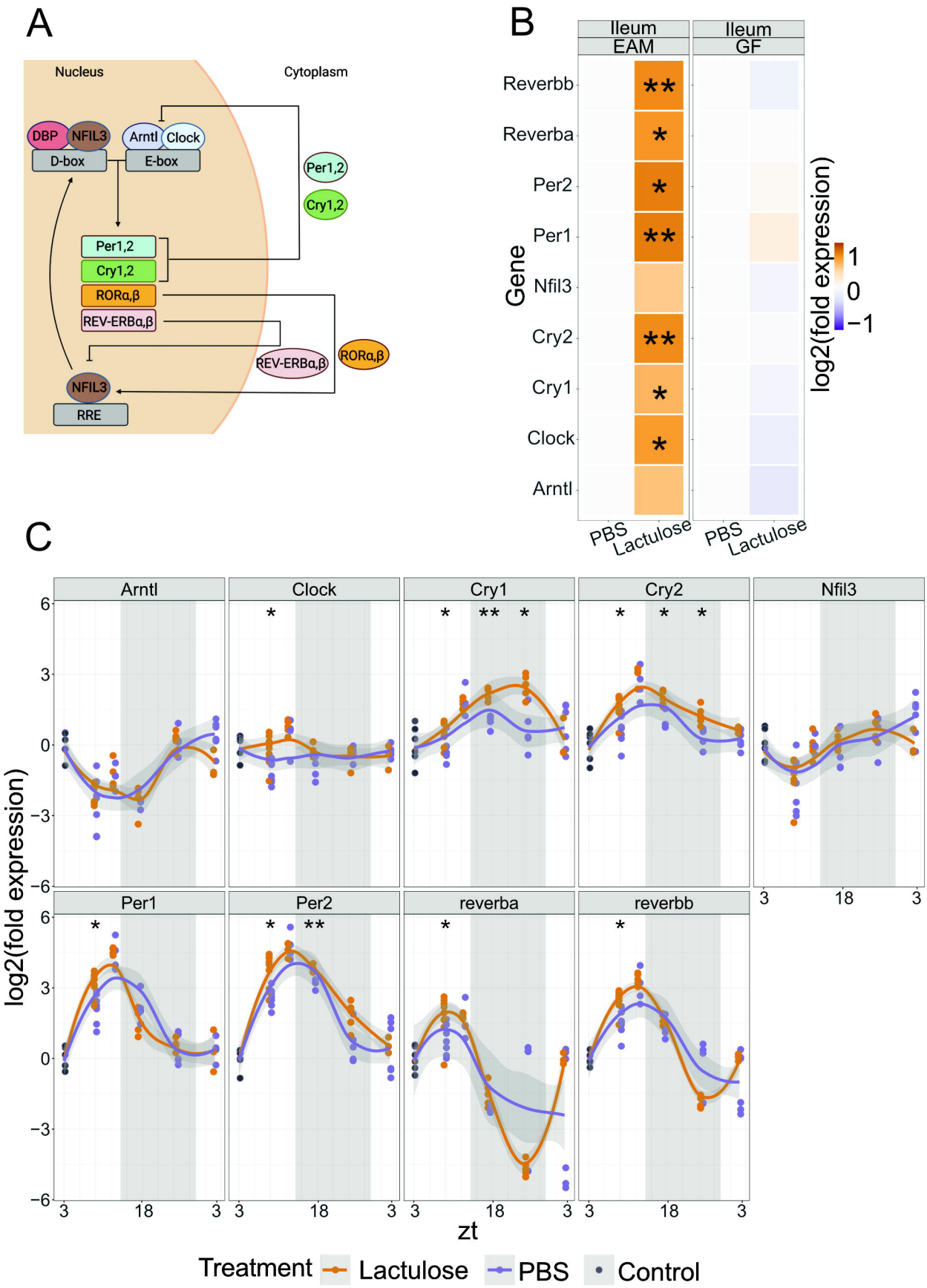

Figure 3: Inducing microbial metabolism acutely alters circadian clock gene expression in small intestinal tissue. A: Schematic of the clock gene network in mice. **B:** Clock gene expression in ileum tissue after EAM mouse treatment (n=17, lactulose=10, PBS=7) and GF mouse treatment (n=16, 8 in each group) measured via RT-PCR. Unpaired T-test revealed increases in EAM gene expression after multiple testing correction ("*" = p<0.05, "**" = p<0.01). **C:** Clock gene expression in EAM mouse ileum tissue over 24 hours after treatment. All gene expression was normalized to samples collected from untreated mice at 9AM (control). Unpaired T-test revealed changes in expression after multiple testing correction ("*"= p<0.05, "**" = p<0.01).

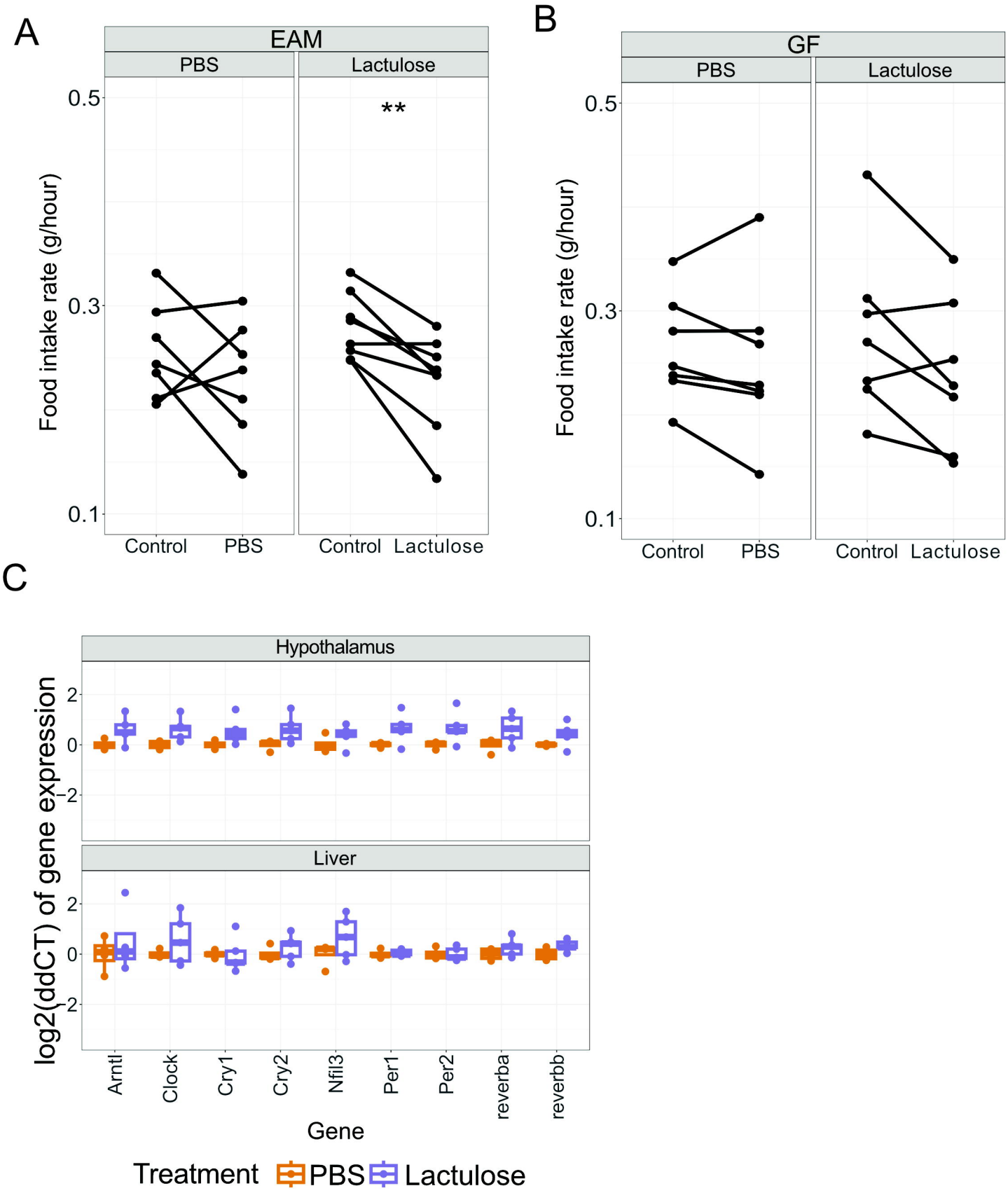

Figure 4: Inducing microbial metabolism decreases host food intake in following active cycle. A: EAM mouse (n=15, lactulose=8, PBS=7) food intake rate in dark phase prior to treatment (control) and following treatment (treatment). Paired T-test displays a reduction in food intake rate after lactulose treatment ($p<0.01$). **B:** GF mouse (n=14, 7 in each group) food intake rate. Paired T-test displays no difference in food intake rate after either treatment. **C:** Clock gene expression in hypothalamus and liver tissues 8 hours after EAM mouse treatment (n=9, lactulose=5, PBS=4) measured via RT-PCR. Unpaired T-test revealed no significant changes in gene expression.

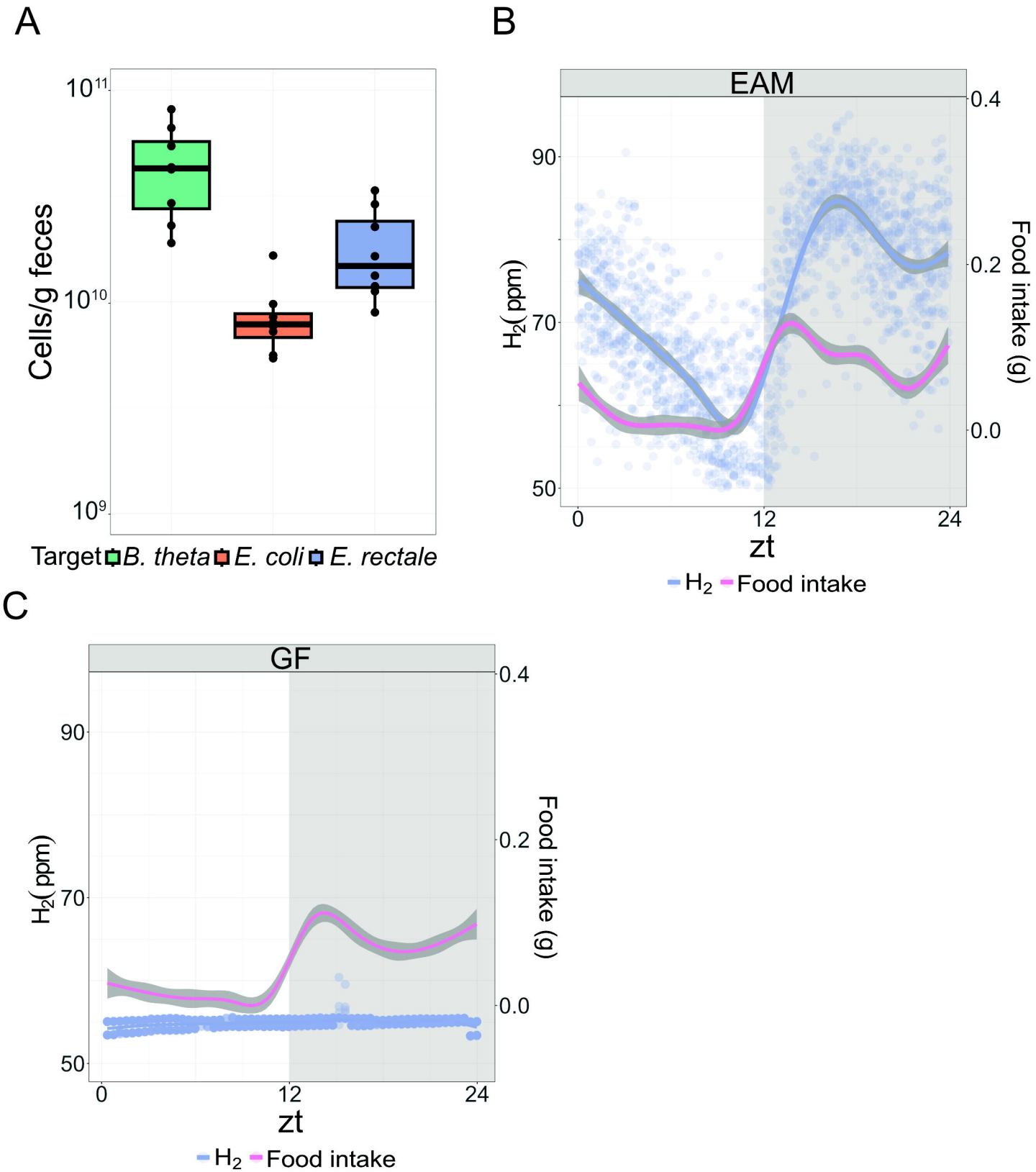

Figure 1: The host circadian rhythm influences microbial cyclical fluctuations. A: Cell counts per grams of feces in the EAM mouse (n=8), calculated by qPCR.**B:** Circadian food intake and hydrogen production of the EAM mouse over two days of measurement, where measurements are taken every 24 minutes (n=16). Curve fit was calculated using formula y~s(x; bs="cs). SE is illustrated with grey shading surrounding line. **C:** Circadian food intake and hydrogen production of the GF mouse (n=8).